UCRL-ID-120480

PANAMINT
Containment Data Report

B. Hudson

T. Stubbs

R. Heinle

March 1995

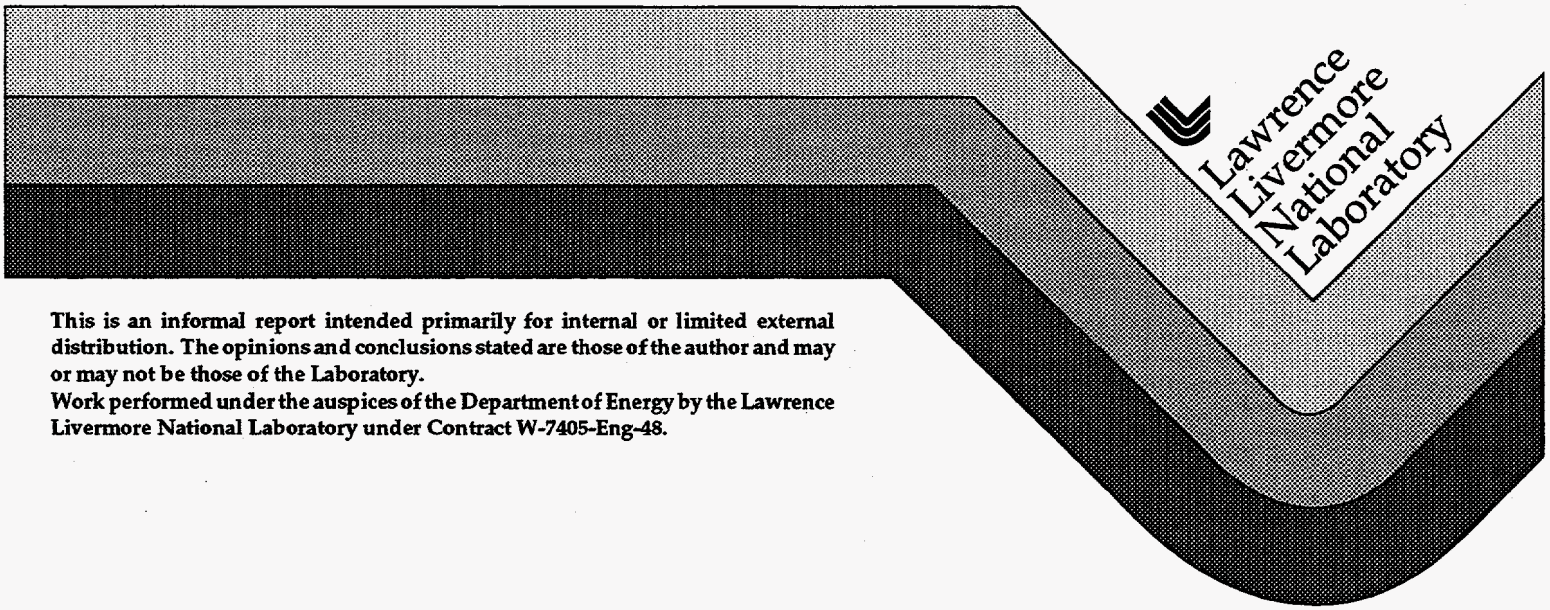

Work performed under the auspices of the Department of Energy by the Lawrence Livermore National Laboratory under Contract W-7405-Eng-48.

PANAMINT Instrumentation Summary

Instrumentation	Fielded	Data Return	Present in this Report
Plug Emplacement	yes	yes	yes
Radiation	yes	yes	yes
Pressure			
Stemming	yes	yes	yes
Challenge	yes	yes	yes
Cavity	no	-	-
Atmospheric	yes	yes	yes
Motion			
Free field	no	-	-
Surface	yes	yes	yes
Plug	yes	yes	yes
Stemming	yes	yes	yes
Surface casing	yes	yes	yes
Emplacement pipe	no	-	-
Recording trailer	yes	yes	yes
Hydroyield [a]	yes	yes	no
Collapse [b]	yes	yes	yes
Stress	yes	yes	yes
Strain [c]	yes	yes	yes
Other Measurements [d]	yes	yes	yes

(a) CORRTEX in emplacement hole.
(b) EXCOR in emplacement hole.
(c) On emplacement pipe during stemming
(d) Displacement array between casing and plug

Event Personnel

Containment Physics	
B. Hudson	LLNL
C. Sisemore	LLNL
J. Kalinowski	EG&G/AVO
T. Stubbs	EG&G/AVO

Instrumentation	
C. Cordill	LLNL
T. Brown	EG&G/AVO
L. Farthing	EG&G/NVO
W. Webb	EG&G/NVO

Contents

1. Event Description

1.1 Containment summary

The PANAMINT event was detonated in hole U2gb of the Nevada Test Site (see figure 1.1) at 13:59 PDT on May 21, 1986. A sub–surface collapse and stemming fall above the bottom plug occurred at about 18.6 minutes after detonation. No radiation arrivals were detected above the ground surface and PANAMINT containment was satisfactory.

1.2 Site

A geologic map showing some of the surface features near the U2gb site is shown in Figure 1.2. The device had a burial depth of 480 m in the Rainier Mesa member of Area 2, about 50 m above the static water level (SWL). The corresponding geologic cross sections are shown in figure 1.3[1].

Stemming of the 2.44 m diameter emplacement hole followed the plan shown in figure 1.4. A log of the stemming operations was maintained by Holmes & Narver, Inc.[2].

1.3 Instrumentation

Figure 1.5 shows a schematic layout of the instrumentation designed to monitor stemming emplacement and performance. Emplacement of each of the three sanded gypsum concrete (SGC) plugs was monitored with temperature and conductivity probes. Stemming performance was monitored by pressure and radiation probes above and below each of the four central plugs.

The pressure challenging the bottom plug was monitored through a hose that extended from the coarse stemming above the plug to below the plug. Pressure transducers were fielded on the hose at its top and in the plug near its bottom. Three sensitive pressure gauges were fielded in the stemming column as shown in figure 1.6 and one was placed 0.61 m in the ground surface, 15.24 m from surface ground zero. These were a part of a continuing study of the pre– and post– event permeability of the emplacement structure and geologic formations of the Nevada Test Site. For about two months before the event, signals from these stations were digitized through a Waveteck® system and recorded on disk by a LSI 11/23 computer.

Hydrodynamic yield of the device , as well as chimney formation, were monitored by two CORRTEX/EXCOR cables (figure 1.5). Results of the hydrodynamic yield measurements are reported elsewhere[3].

Vertical motion was monitored in the stemming, in the top three plugs and in the ground surface at ranges of 14.75 and 15.61 m from Surface Ground Zero (SGZ). Triaxial motion of the recording trailer was also measured. A proximity switch array was mounted in the top plug at the location of the bottom of the surface casing to detect relative motion between the plug and casing. Motion of the gas sample hose relative to the skid was monitored by a rotary potentiometer mounted between the two.

A new version of a fluid–coupled stress gauge[4] was tested at two locations in the bottom stemming plug.

Brief histories of the instrumentation set–up and fielding operations are given in references 5 and 6.

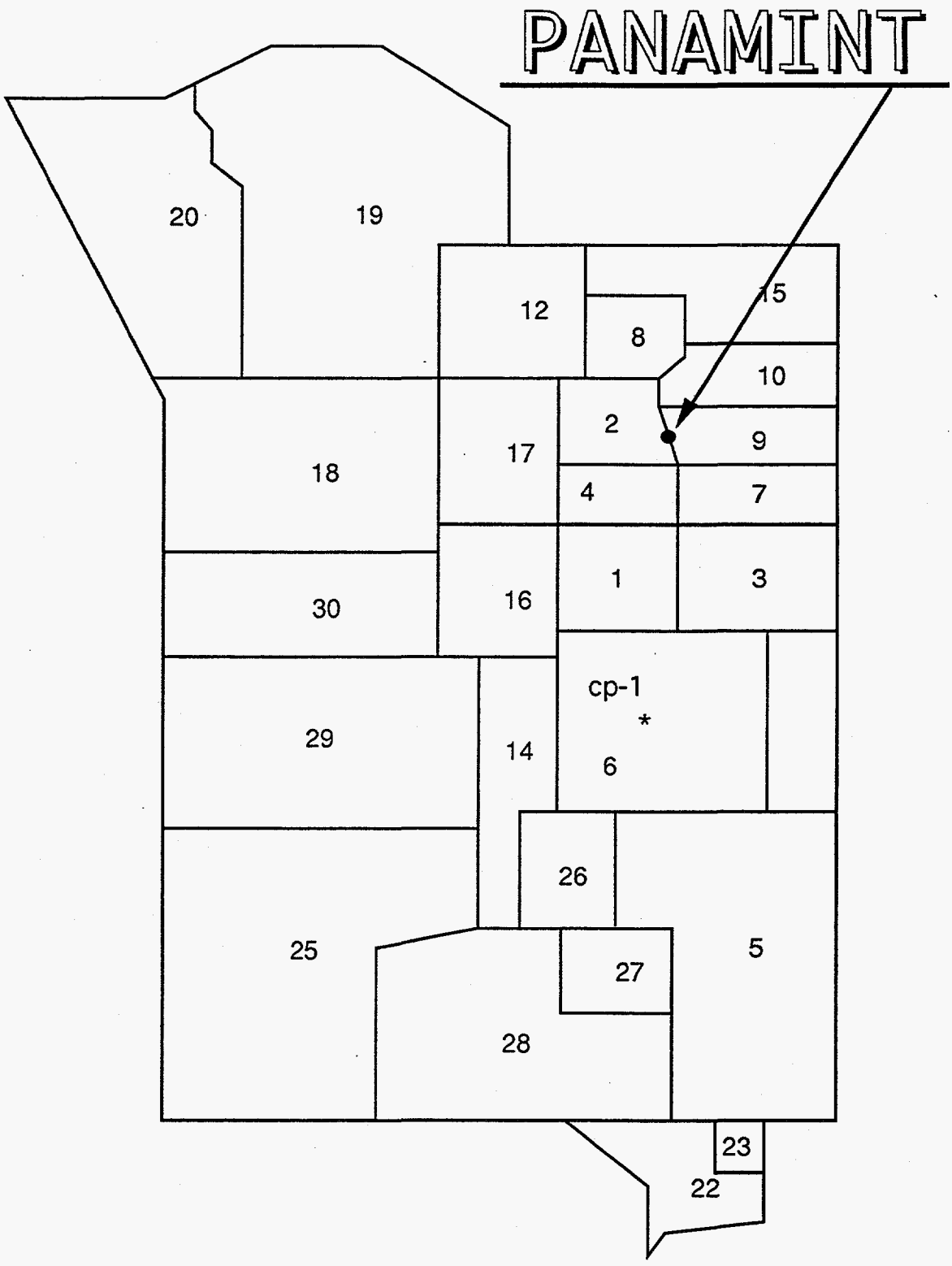

Figure 1.1 Map of the Nevada Test Site indicating the location of hole U2gb.

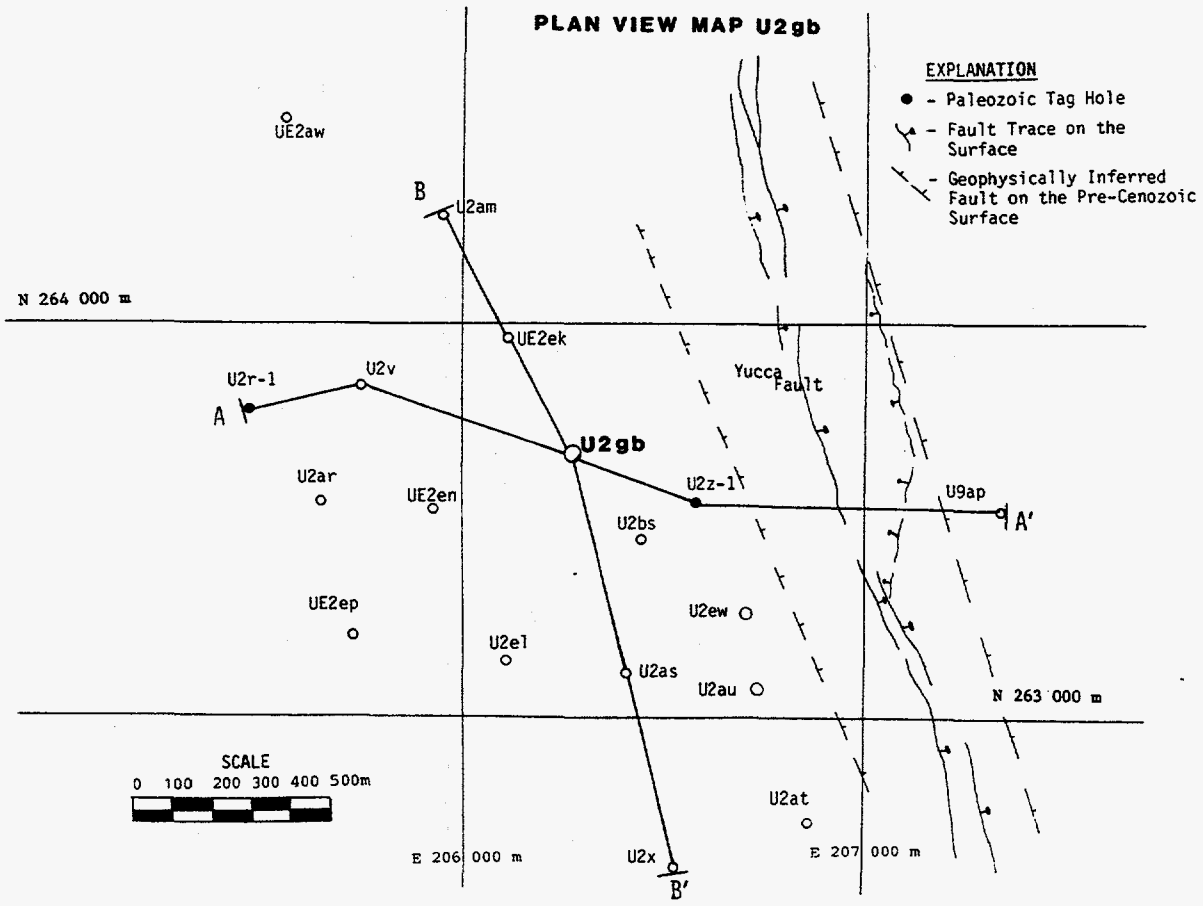

Figure 1.2 Plan map for geologic cross sections through hole U2gb.

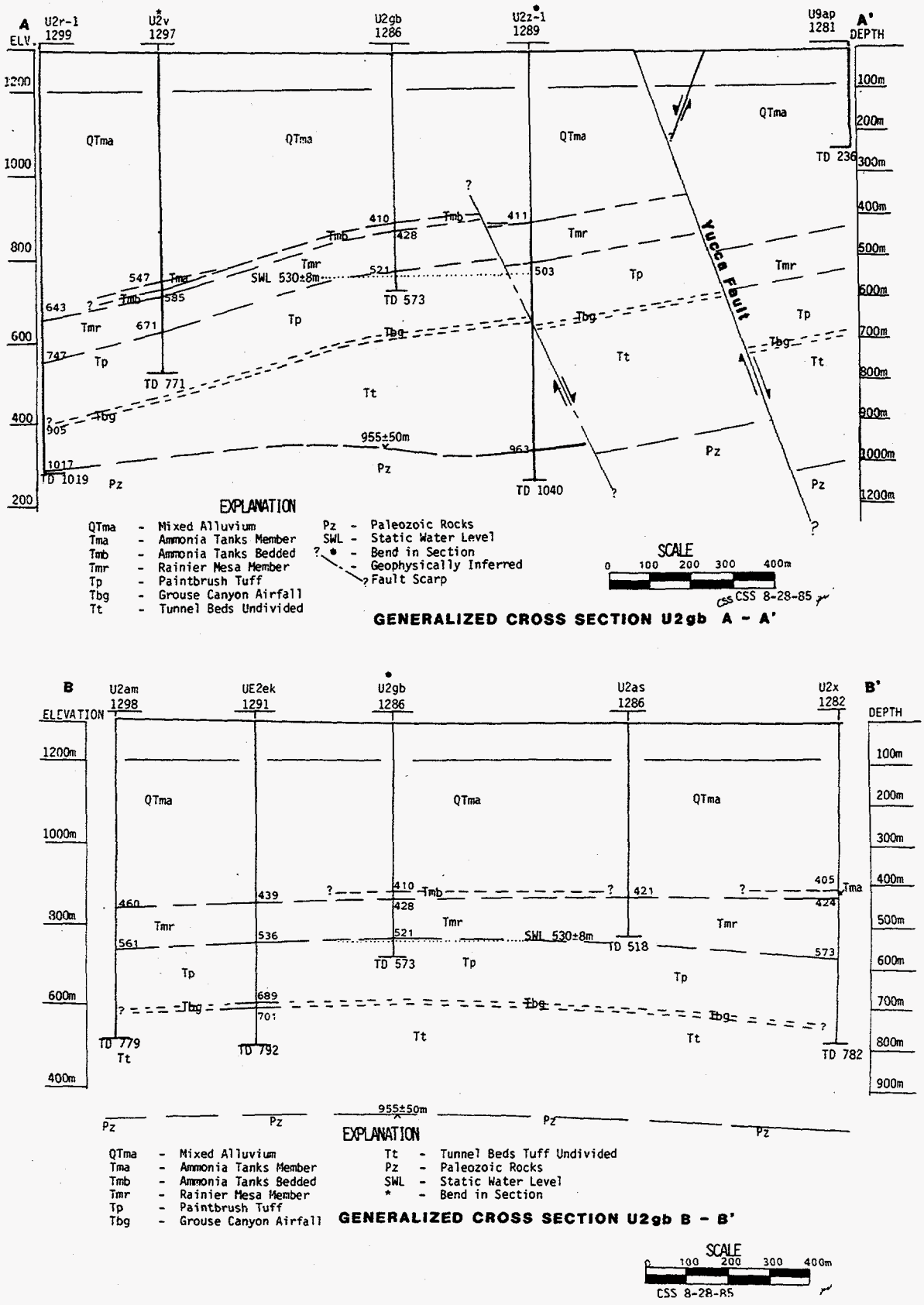

Figure 1.3 Geologic cross sections through hole U2gb. A site description is given in reference 1.

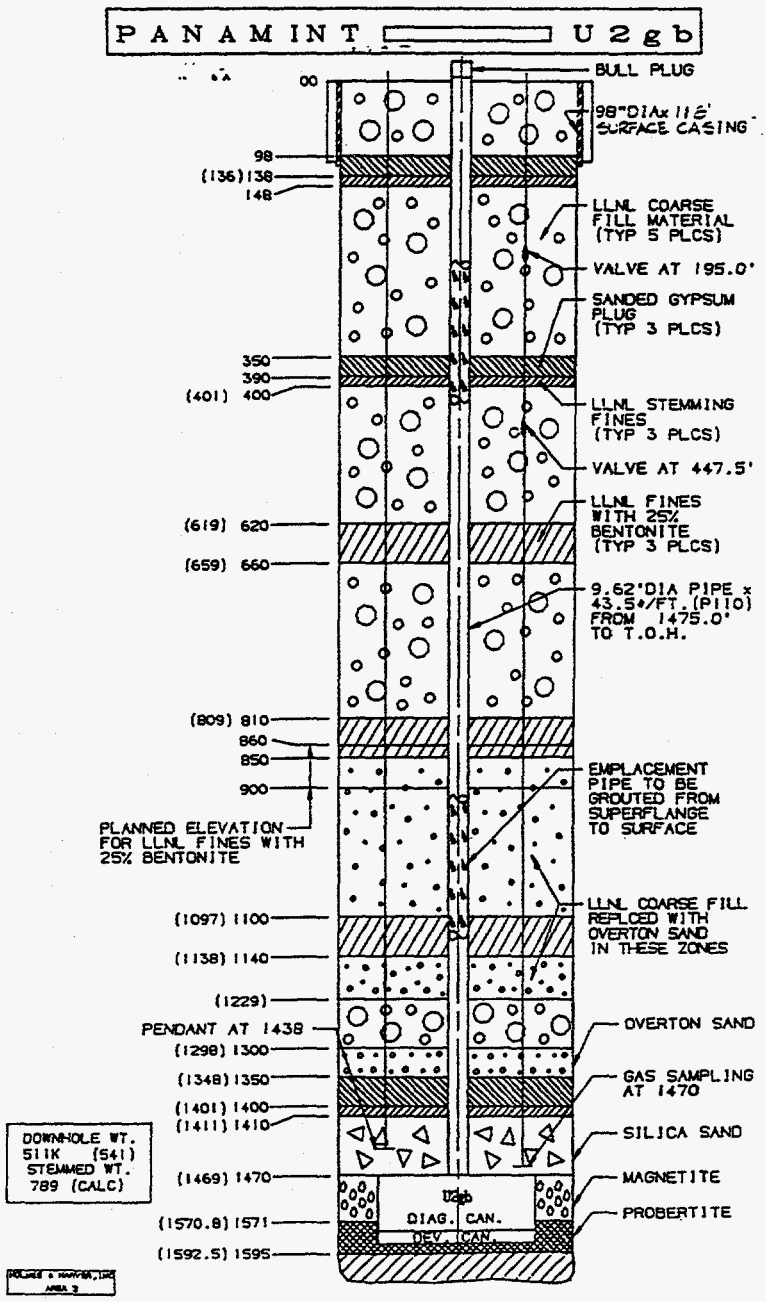

Figure 1.4 As-built stemming plan for hole U2gb, the PANAMINT event emplacement hole.

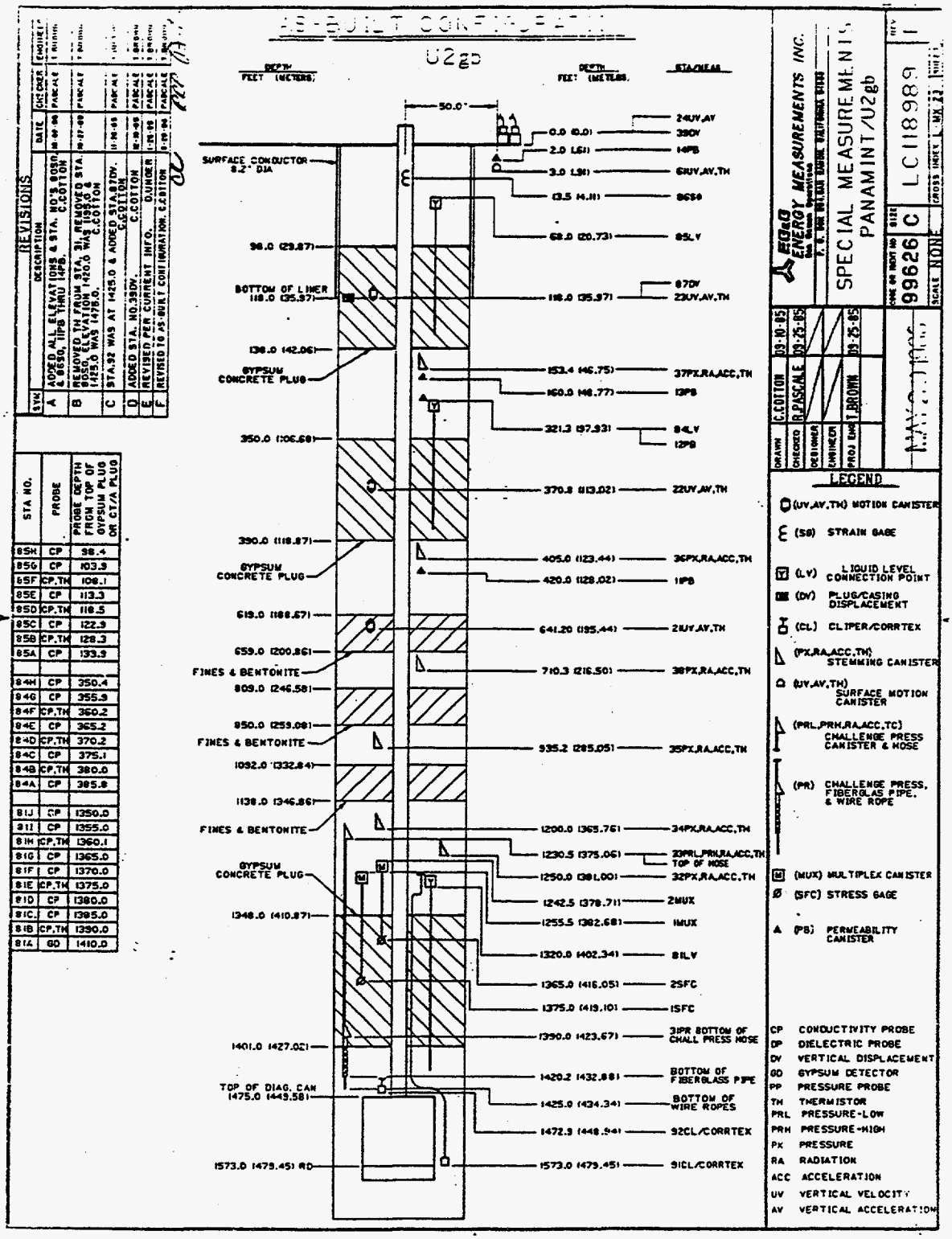

Figure 1.5 As-built containment instrumentation plan for U2gb, the PANAMINT event emplacement hole.

2. Emplacement

2.1 Pipe strain

The emplacement pipe was instrumented for strain with a pair of gauges on the final pipe section below the load collar (station 86). Strain gauge #1 failed and figure 2.1 shows the strain history recorded from strain gauge #2 between the time of landing of the device and the emplacing the first plug. No further data survive.

2.2 Plug levels and temperature

The emplacement of each of the three SGC plugs was monitored with conductivity and temperature probes at locations tabulated in figure 1.5. Figures 2.2–2.4 show plots of the SGC emplacement and temperature histories. The temperature histories were digitally recorded on floppy disks which, apparently, did not survive until the data could transcribed to a more permanent medium. Proper curing of the cement was assured during stemming by the field personnel, but no histories are presented here. As shown in figure 1.5, a series of three layers composed of LLNL fines and bentonite ("fines plugs") were included in the coarse stemming between the two deepest SGC plugs. All plugs were emplaced as planned.

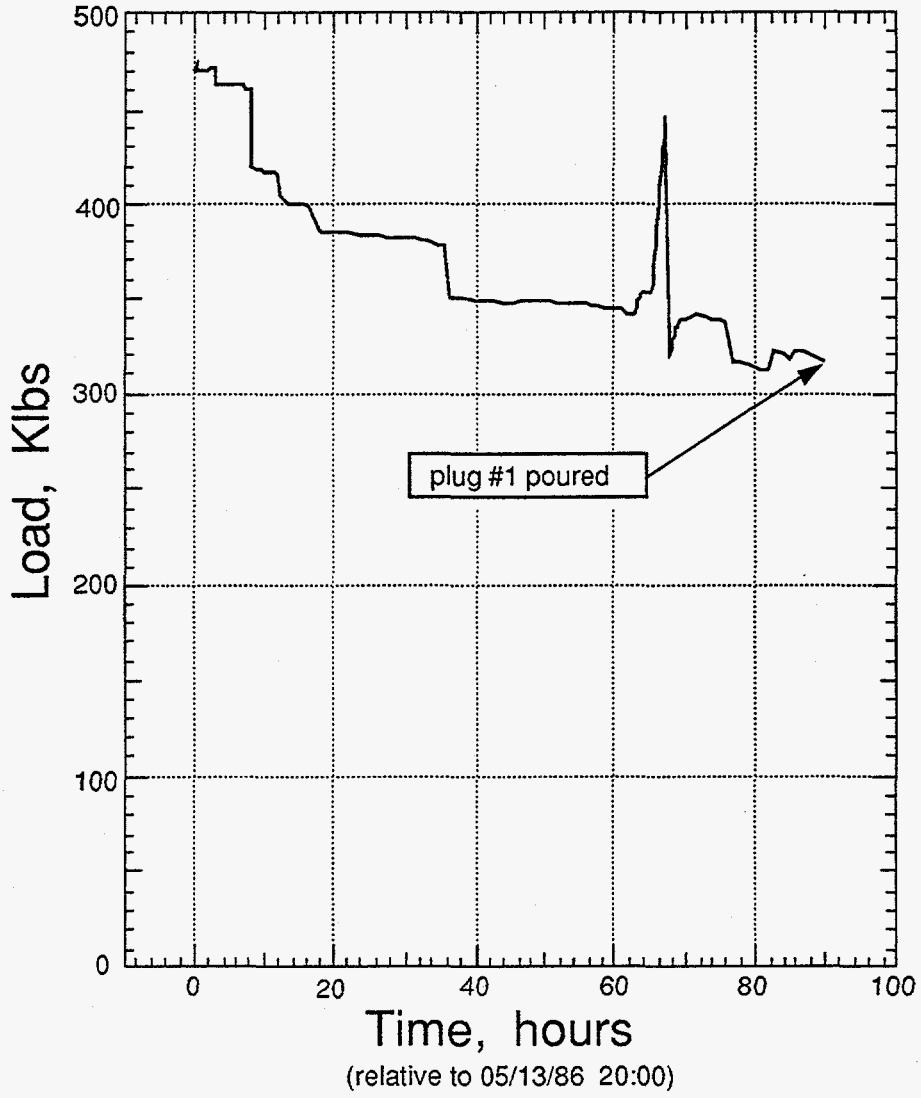

Figure 2.1 Emplacement pipe strain history at station 86 during stemming.

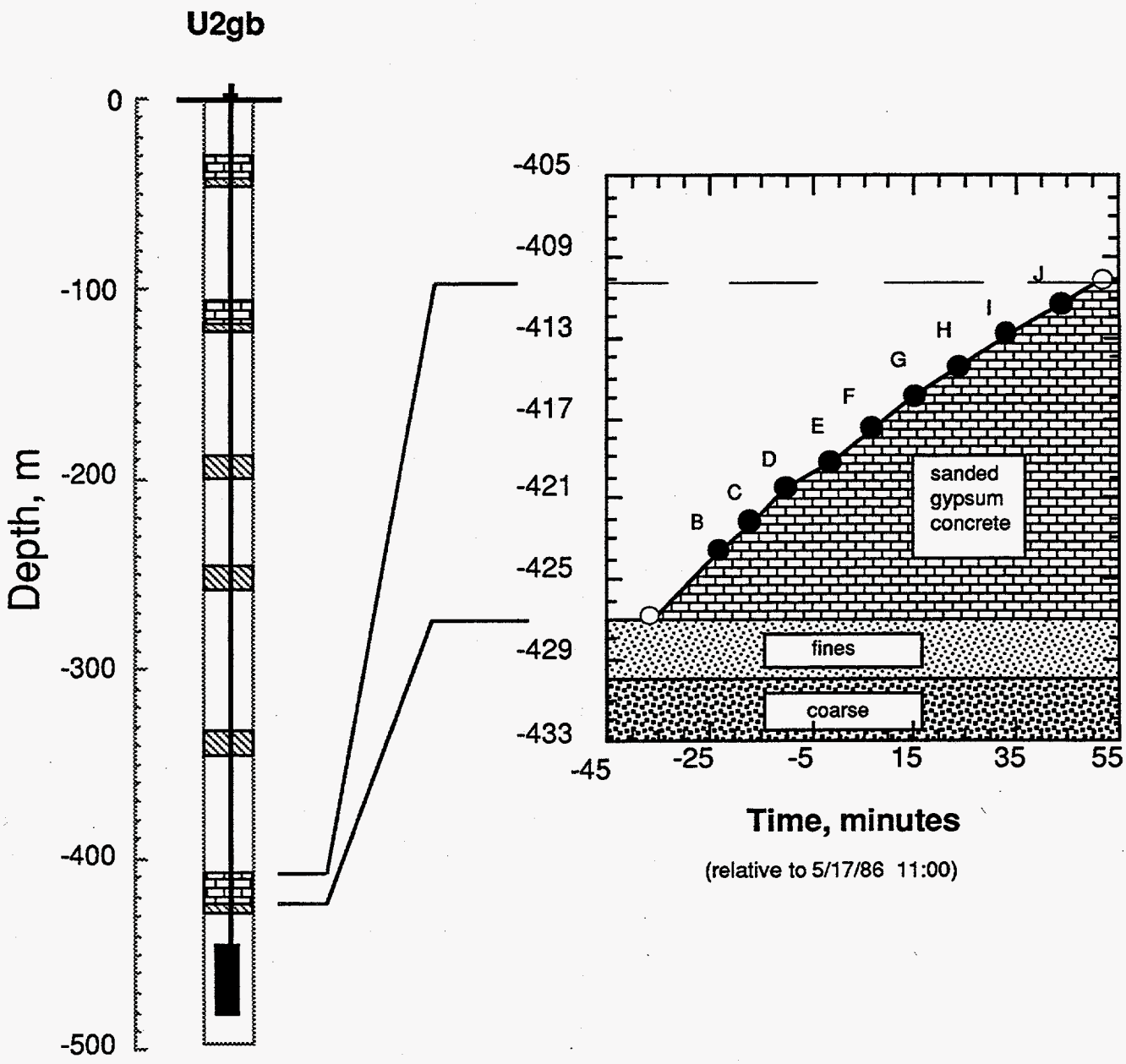

Figure 2.2 Sanded gypsum emplacement for the first plug. The upper and lower plug boundaries were determined with a tag line (open circles); solid symbols indicate the probe elevations. Probes labeled B, E, and H included temperature sensors (temperature histories are not available).

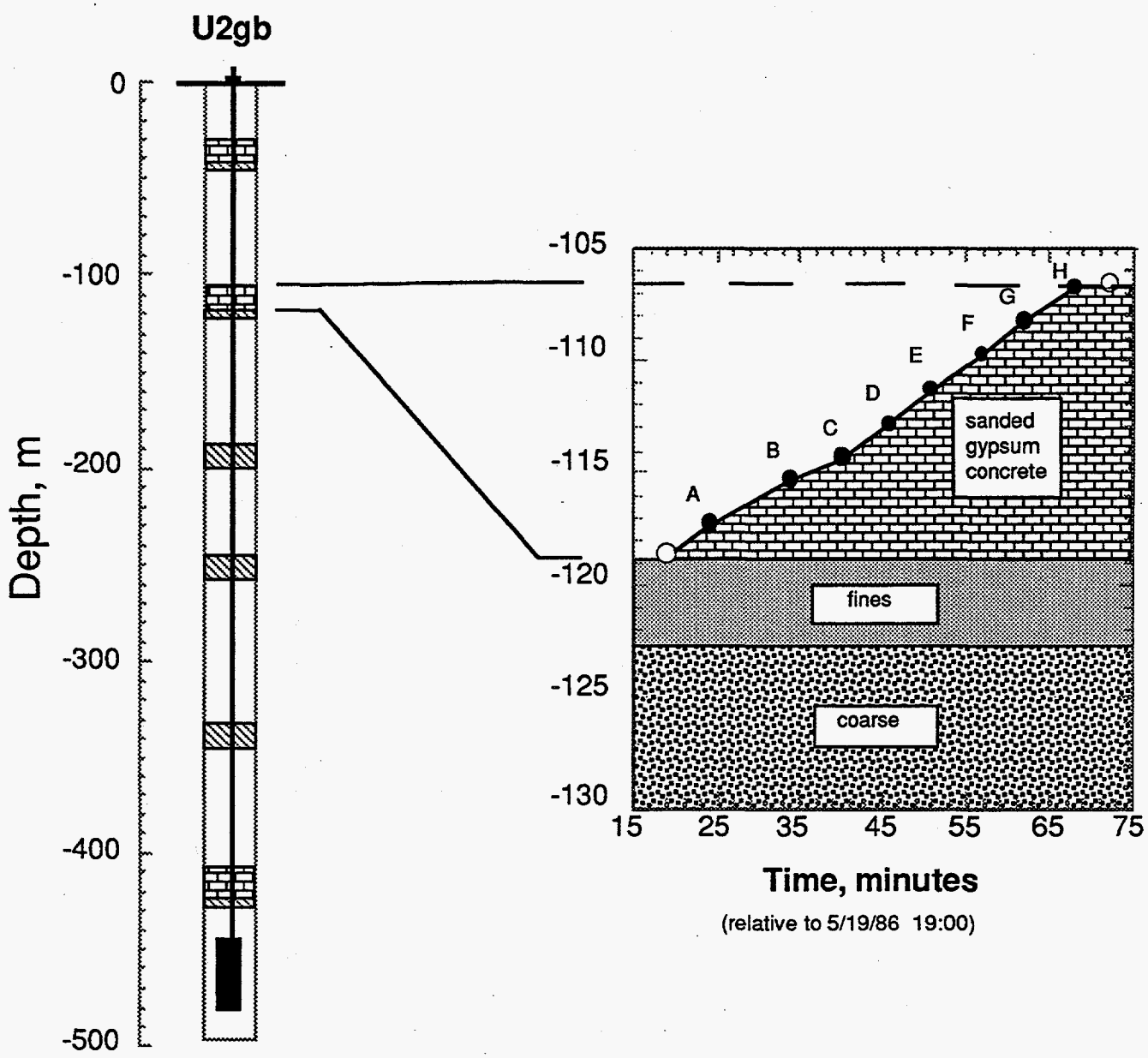

Figure 2.3 Sanded gypsum emplacement for the fifth plug. The upper and lower plug boundaries were determined with a tag line (open circles); solid symbols indicate the probe elevations. Probes labeled B, D, and F included temperature sensors (temperature histories are not available).

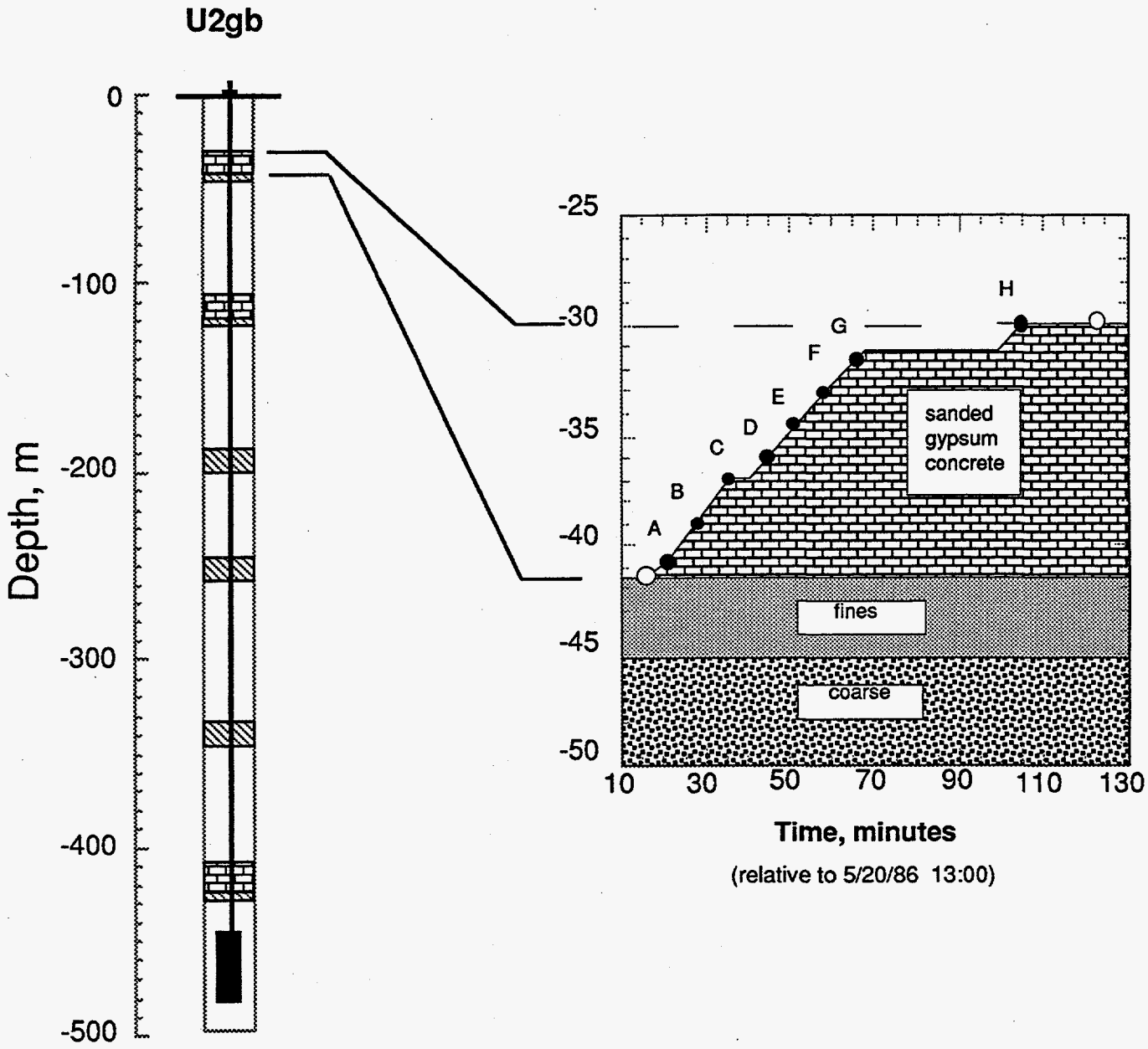

Figure 2.4 Sanded gypsum emplacement for the sixth plug. The upper and lower plug boundaries were determined with a tag line (open circles); solid symbols indicate the probe elevations. Probes labeled B, D, and F included temperature sensors (temperature histories are not available).

3. Stemming Performance

3.1 Pressure and radiation

As indicated in Figure 1.4, the region between each of the stemming plugs was monitored by pressure and radiation stations The analog signals were transmitted up–hole and then recorded on magnetic tape in the recording trailer.

The pressure challenging the bottom plug was measured at station 33 (mounted between the first and second plugs and connected to the region below the first plug through a hose extending to below the first plug). A second pressure transducer (station 31) was mounted within and near the bottom of the bottom plug and was also connected to the hose.

Figures 3.1–3.8 show the pressure and radiation histories from a few minutes before detonation to more than eleven hours later or until the station signal was lost. As shown in figure 3.1, station 31 (located at the bottom of the deepest SGC plug) was lost soon after shock arrival. Station 33 (on the top of the challenge pressure hose) was lost at collapse (about 1118 s) and the remainder of the pressure and radiation transducer channels continued to provide information as long as the recording system was active.

3.2 Motion

Figures 3.9–3.19 show the first six seconds of explosion-induced vertical motion as measured in the emplacement hole. Station 61 monitored the vertical motion of the ground surface at a depth of 0.91 m and a horizontal range of 15.24 m from SGZ. Explosion–induced data derived from this station are shown in figure 3.20. The vertical motion of the recording trailer (station 71) is shown in figure 3.21.

Characteristics of the motion are given in table 3.1 and characteristics of the motion transducers are given in tables 3.2 and 3.3.

A vertical, linear array of seven proximity switches was mounted in the top SGC plug next to the bottom of the surface casing. Switch states of "on" imply the nearby presence of ferrous metal (surface casing) and "off", its absence. No relative motion between the top plug and the surface casing was sensed at any time by this array.

Figures 3.22–3.25 show a comparison between the pressure and the displacement for the first six seconds after detonation for stations 34, 35, and 38, respectively. A stemming slump, triggered by the detonation, is seen to progress to below the fourth plug before three seconds after detonation.

3.3 Collapse

CLIPER information consists of a single datum indicating a cable break at a depth of about 382 m at a time of 1117 s.

A sharp pressure drop at collapse time followed by a long recovery, suggestive of a stemming fall, was seen at stations 32 and 34 (figures 3.2 and 3.4). These two records (along with those of stations 35 and 38) are compared, during the collapse phase, in figure 3.25. The trace from station 32 was left unfiltered to show the full time resolution of the recorded data. Collapse pressure jumps appear to be simultaneous at stations 32 and 34 suggesting that both stations experienced nearly the same stemming behavior. The arrival of radiation at station 32 at the time of collapse and the subsequent jumps in radiation level suggests that the bottom plug was not effective after collapse. Additionally, the level of radiation, its wave form and the wave forms of the pressure at stations 32 and 34 indicate that the stemming between station 32 and 34 remained effective (figures 3.26 and 3.27). Taken together, these data and the CLIPER information suggest that the geologic formation did not collapse much beyond station 32 and that the deepest SGC plug failed upon collapse.

The motion data during collapse are shown in figures 3.28–3.34. The motion channels at stations 32 and 33 failed at about 1118 seconds after detonation, with station 33 preceding 32 by about one second. This may have been caused by an interaction between challenge pressure hose and the SGC of the bottom plug (which appears to have failed). No indication of collapse motion was detected at depths less than 124 m.

Table 3.1 Summary of Motion

Gauge	Slant Range (m)	Arrival Time (ms)	Acceleration Peak (g)	Velocity Peak (m/s)	Displacement Peak (cm)	Displacement Residual (cm)
21av	284.6	93	2.0	0.43	1.6, -7.5	-5
21uv	-	-	-	0.40, -1.0	8., -5.	-8
22av	367.0	107, 198	1.25	0.47	1.8	-1
22uv	-	-	-	0.57	2.2	-1.3
23av	444.0	253	0.80	0.29	1.6	-0.5
23uv	-	-	-	0.48	2.6	-1.5
24av	480.0	192, 270	1.1	0.46	2.4	-2
24uv	-	-	-	0.50	2.7	-2
32av	99.0	50	5.7	1.4	7.9	0.5
33av	104.9	37, 51	5.6	1.4	8.2	2.
34av	114.2	45, 53	2.7	0.24, -2.1	0.5, -37	-37(c)
35av	194.9	60	1.0	0.2, -1.4	0.7, -125	(c)
36av	356,6	109	1.5	0.46	1.8, -2.0	-19
37av	433.3	146	0.95	0.34	1.5	-0.3
38av	263.5	78	2, ±7	0.64, -0.95	2.8, -23	-2., -22.
61av	480.3	292	1.8	0.70	5.0	-2.8(d)
61uv	-	-	-	0.87	6.0	-2.2
71av	537(d)	330	2.0, 4.0(b)	0.85	8.0	-3
71uv	-	-	-	0.90	8.4	-2.5

(a) Emplacement pipe or strongback–stemming interaction.
(b) Slap-down peak.
(c) Signal lost early (before 2 s.): this value inaccurate or not available.
(d) Approximate.

Table 3.2 Accelerometer Characteristics

Gauge	Natural Frequency (Hz)	Damping Ratio	System Range (g's)
21av	230	0.75	8
22av	240	0.75	10
23av	390	0.65	15
24av	320	0.65	20
32av[(a)]	2500	0.7	200
33av[(a)]	2500	0.7	200
34av[(a)]	750	0.7	50
35av[(a)]	750	0.7	20
36av[(a)]	750	0.7	20
37av[(a)]	750	0.7	50
38av[(a)]	750	0.7	20
61av	410	0.65	20
71av	325	0.65	20

(a) Piezo–resistive elements; manufacturers specifications

Table 3.3 Velocimeter Characteristics

Gauge	Natural Frequency (Hz)	Time to 0.5 Amplitude (s)	Calibration Temperature (^{o}C)	Operate Temperature (^{o}C)	System Range (m/s)
21uv	3.562	8.88	25.26	20.32	8
22uv	3.509	8.27	25.64	39.27	8
23uv	3.584	8.66	24.39	43.22	8
24uv	3.582	8.58	25.91	14.31	8
61uv	3.613	8.66	24.84	16.24	8
71uv	2.999	23.50	24.34	18.61	7

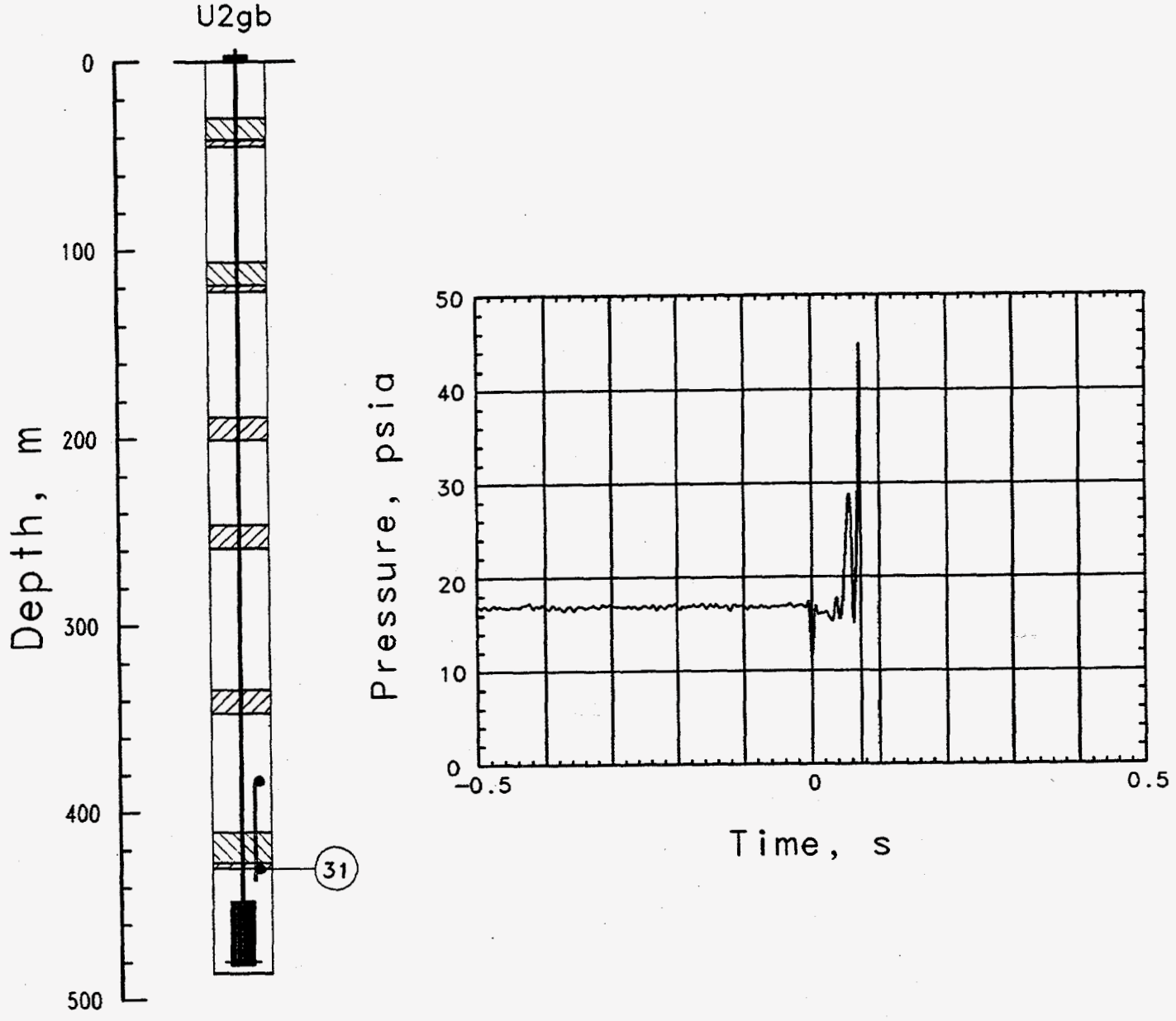

Figure 3.1 Challenge pressure as measured below the first SGC plug (station 31). This station failed shortly after shock arrival time.

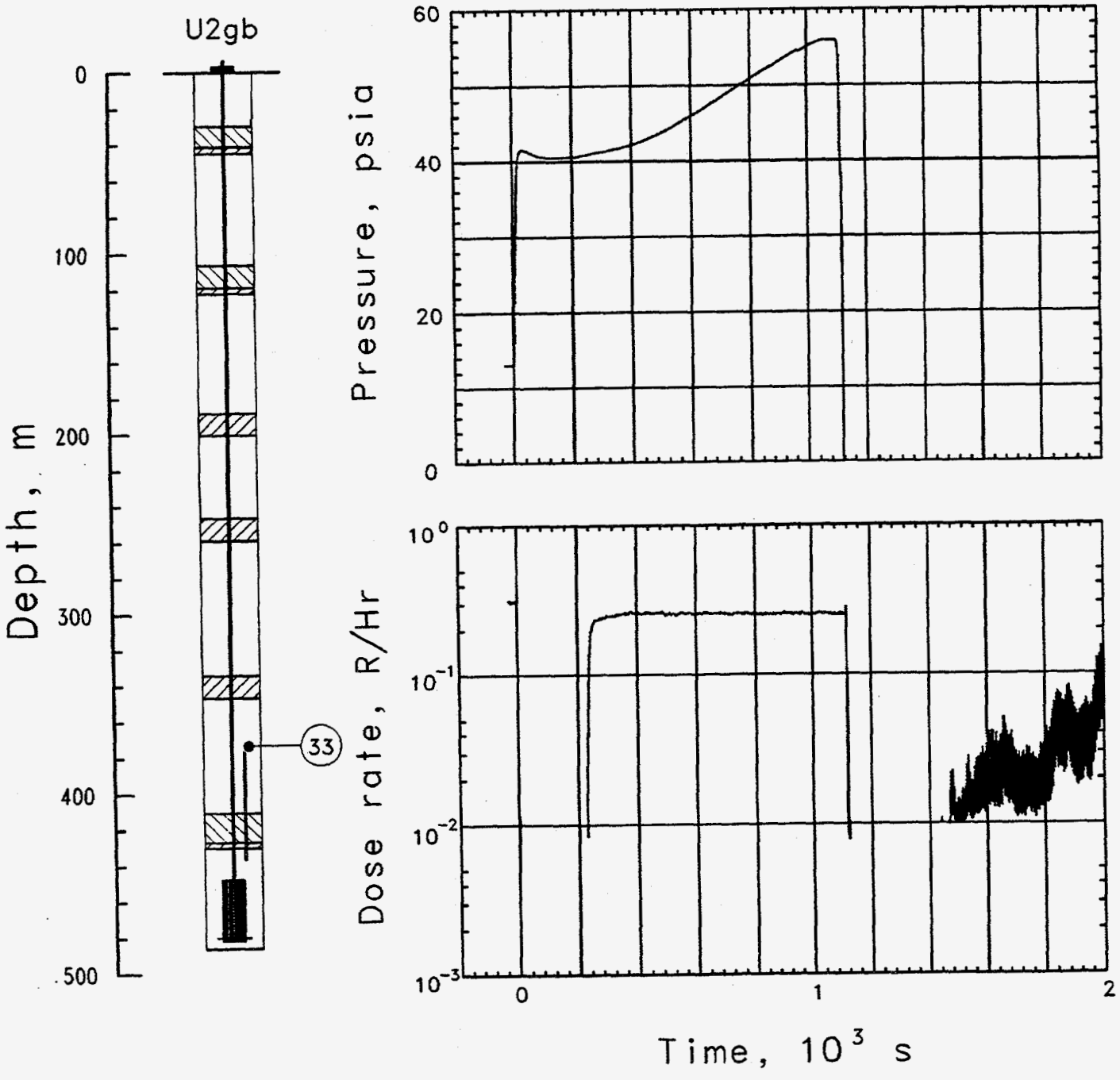

Figure 3.2 Challenge pressure measurements in the hose through the first SGC plug (station 33). All signals from this station were lost at collapse time (1118 s). Although radiation was also monitored, it was apparently not transported through the hose to the detector.

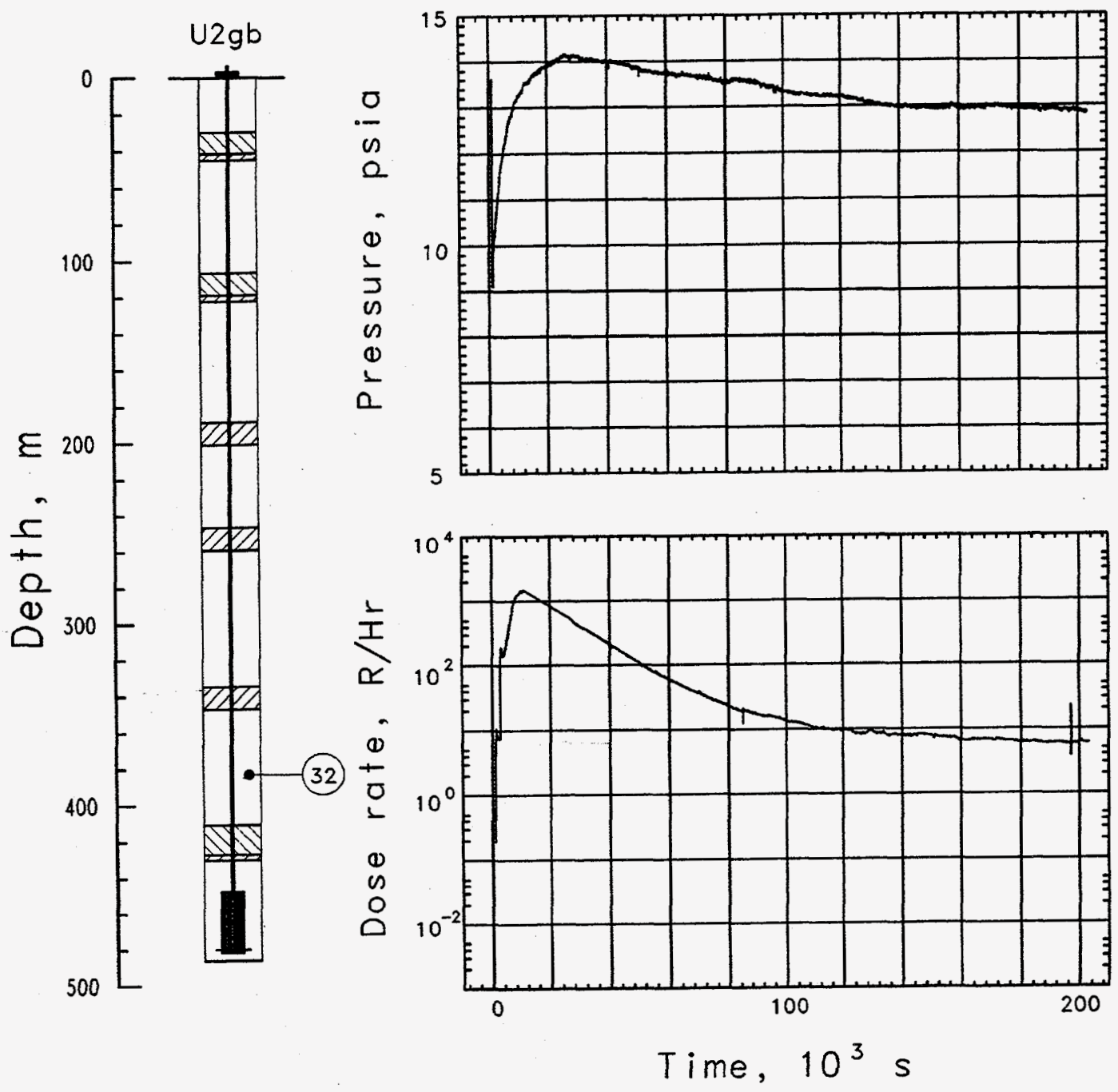

Figure 3.3 Pressure and radiation histories measured in the coarse stemming above the first SGC plug (station 32 at 381 m depth). These data indicate an arrival of radioactive material at collapse time (1118 s). The radiation appears to arrive discontinuously after this, suggesting a stemming fall.

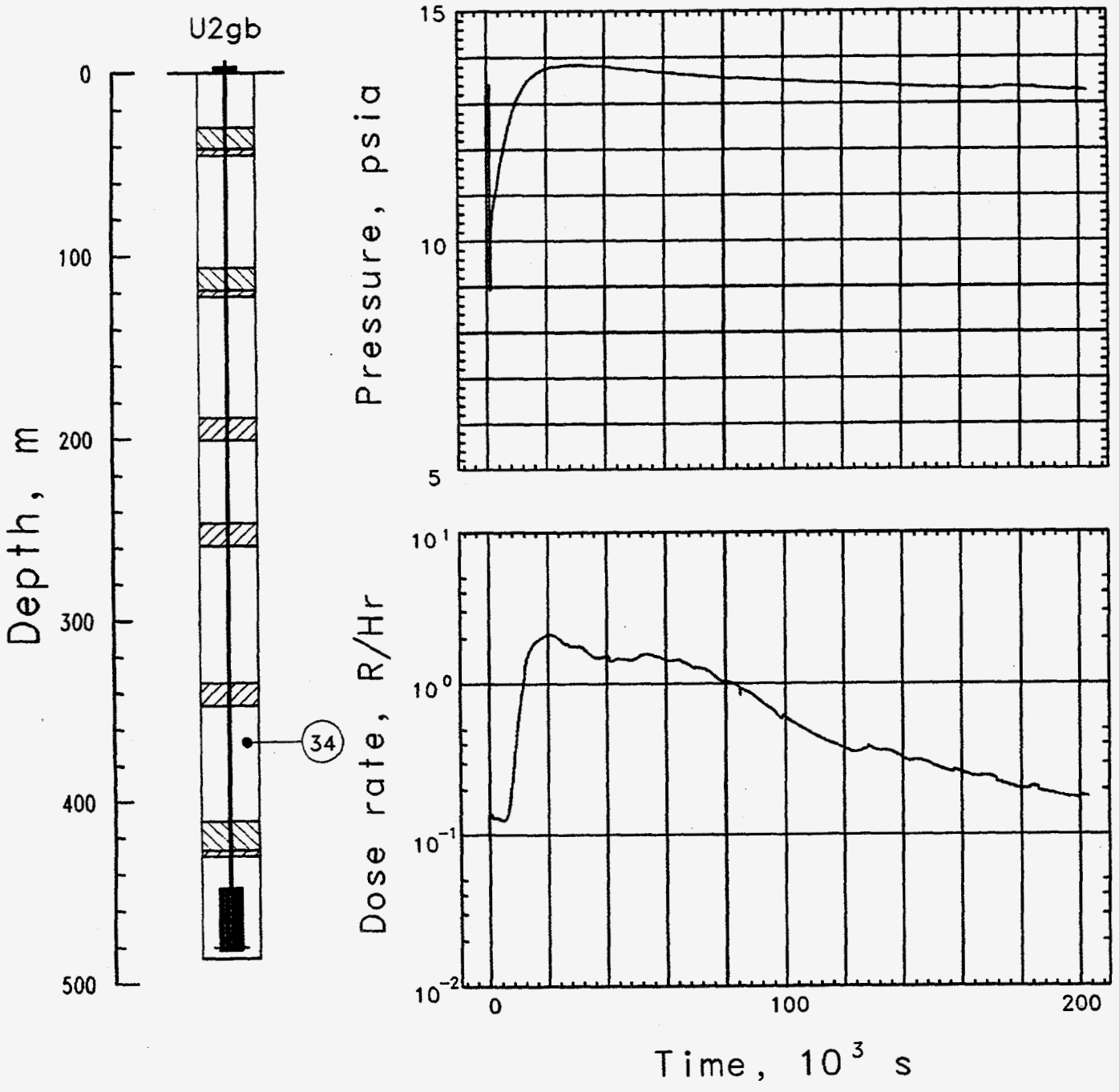

Figure 3.4 Pressure and radiation histories measured in the coarse stemming below the second plug (station 34 at 365.8 m depth). This plug was composed of LLNL fines. Radiation appears to arrive at about 5400 s.

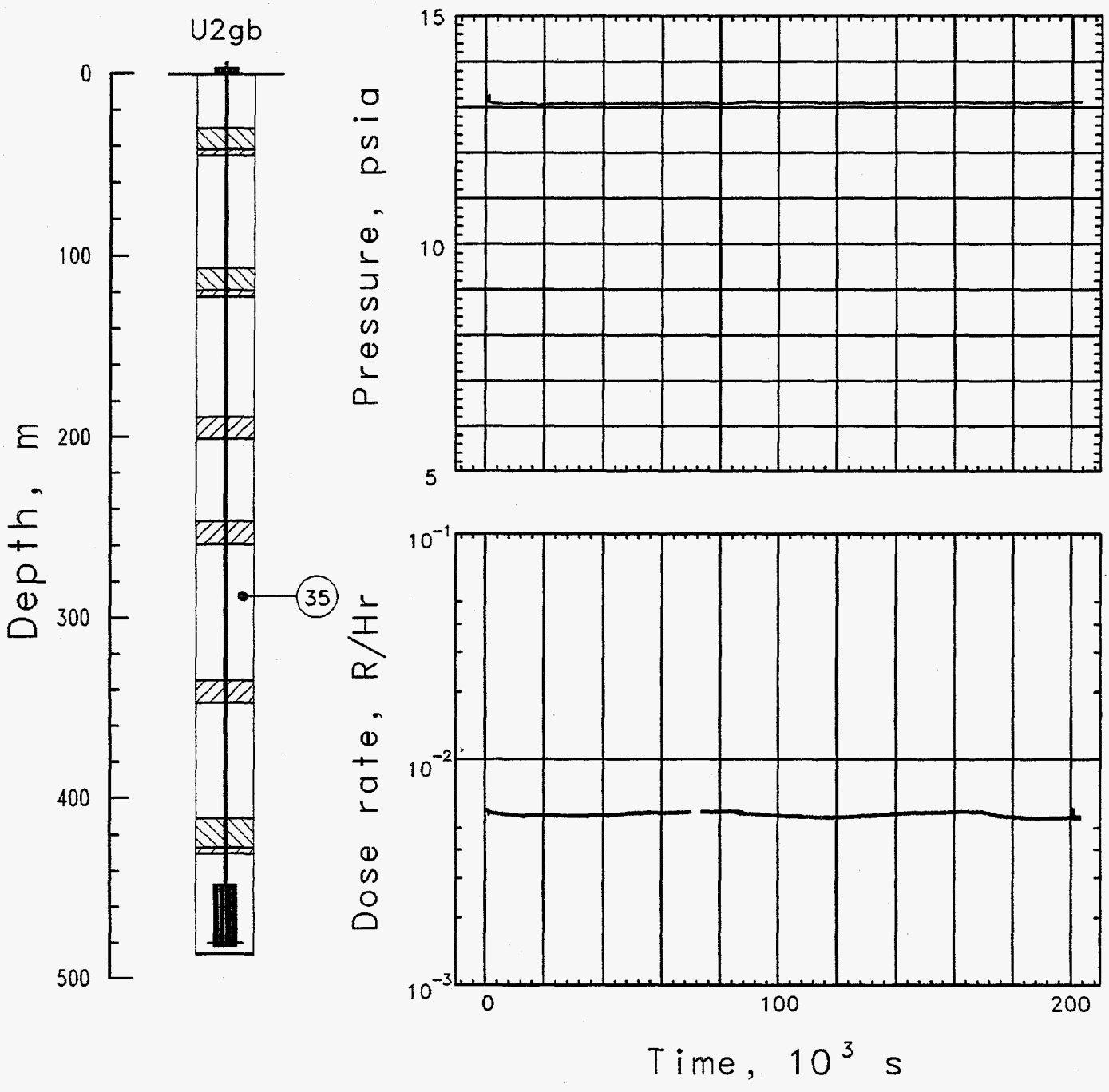

Figure 3.5 Pressure and radiation histories measured in the coarse stemming below the third plug (station 35 at 285.1 m depth). This plug was composed of LLNL fines. No radioactive material arrivals were observed at or above this station.

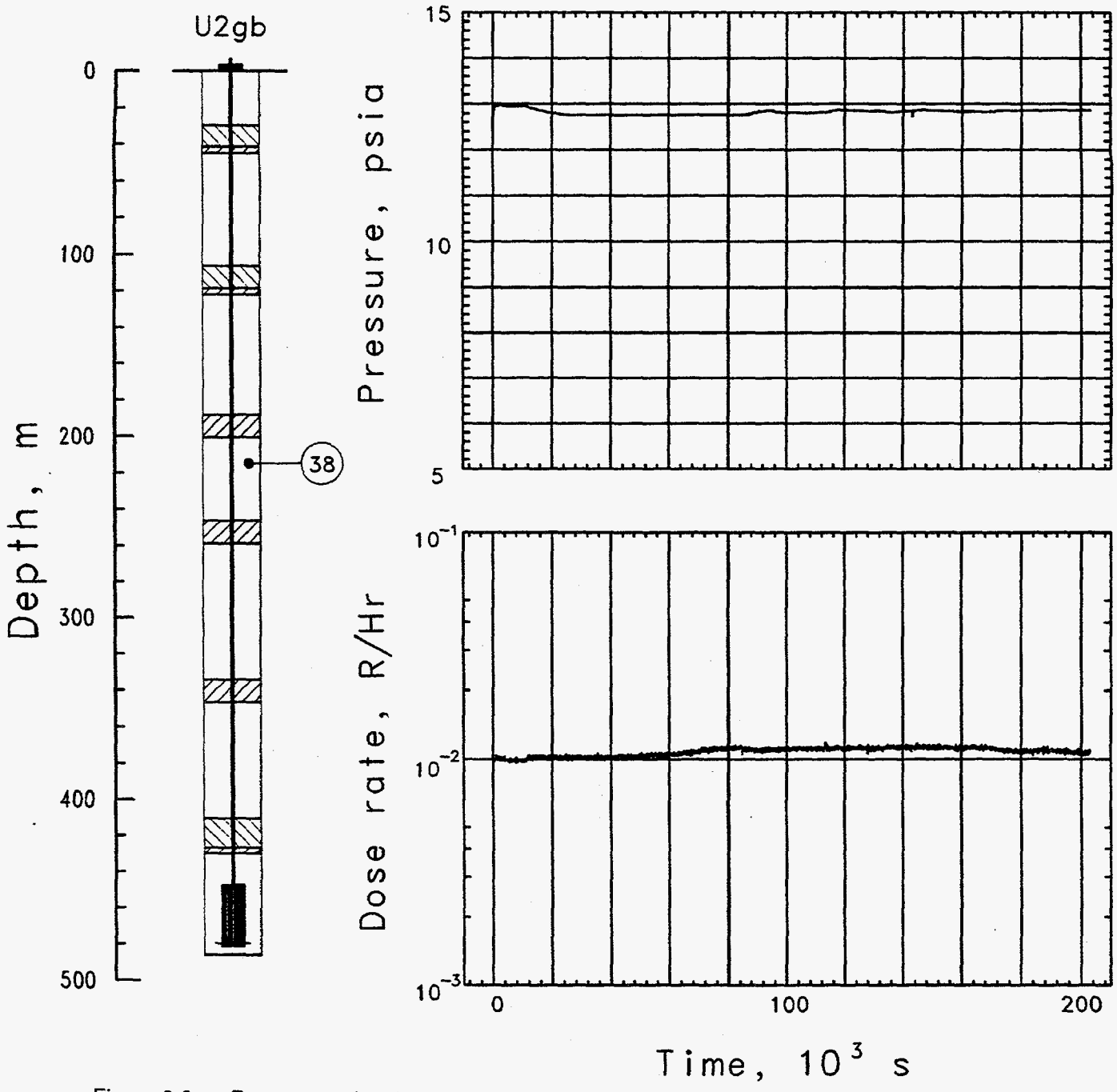

Figure 3.6 Pressure and radiation histories measured in the coarse stemming below the fourth plug (station 38 at 216.5 m depth). This plug was composed of LLNL fines. A possible arrival is observed at about 50,000 s. No radiation arrivals were observed above this station.

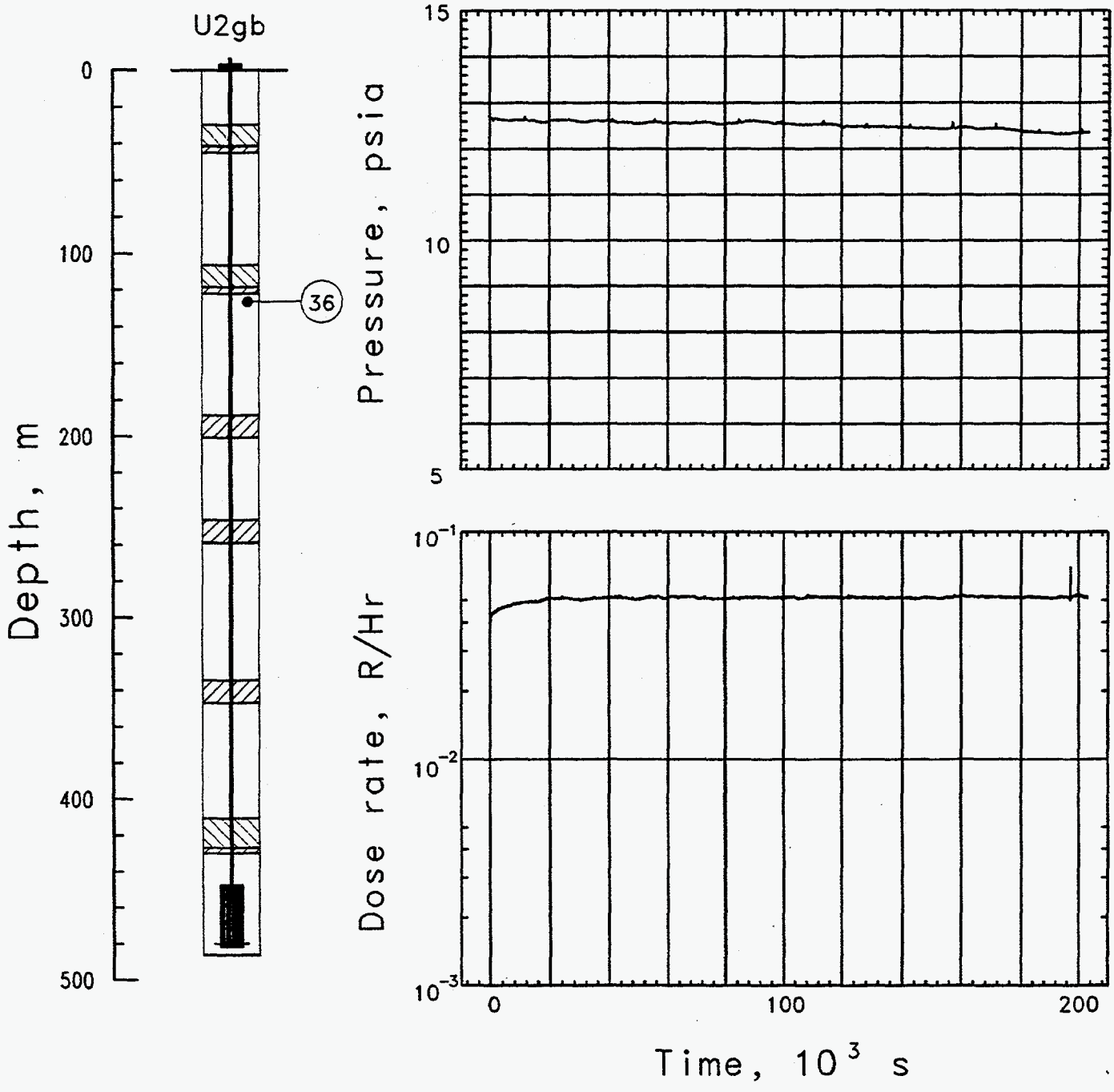

Figure 3.7 Pressure and radiation histories measured in the coarse stemming below the fifth plug (station 36 at 132.4 m depth). This plug was composed of SGC. No radioactive material arrivals were observed at or above this station.

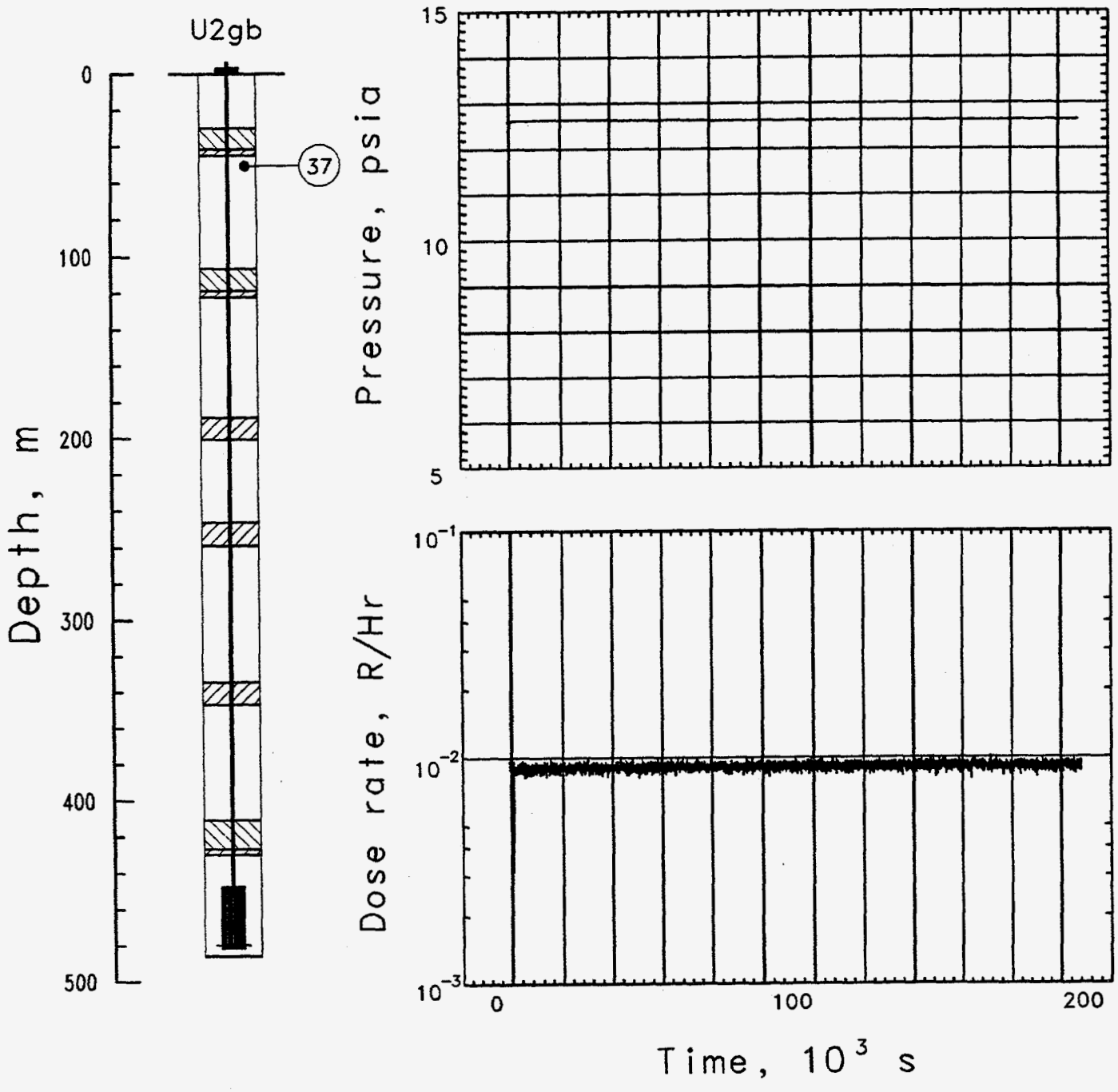

Figure 3.8 Pressure and radiation histories measured in the coarse stemming below the top plug (station 37 at 46.8 m depth). This plug was composed of SGC.

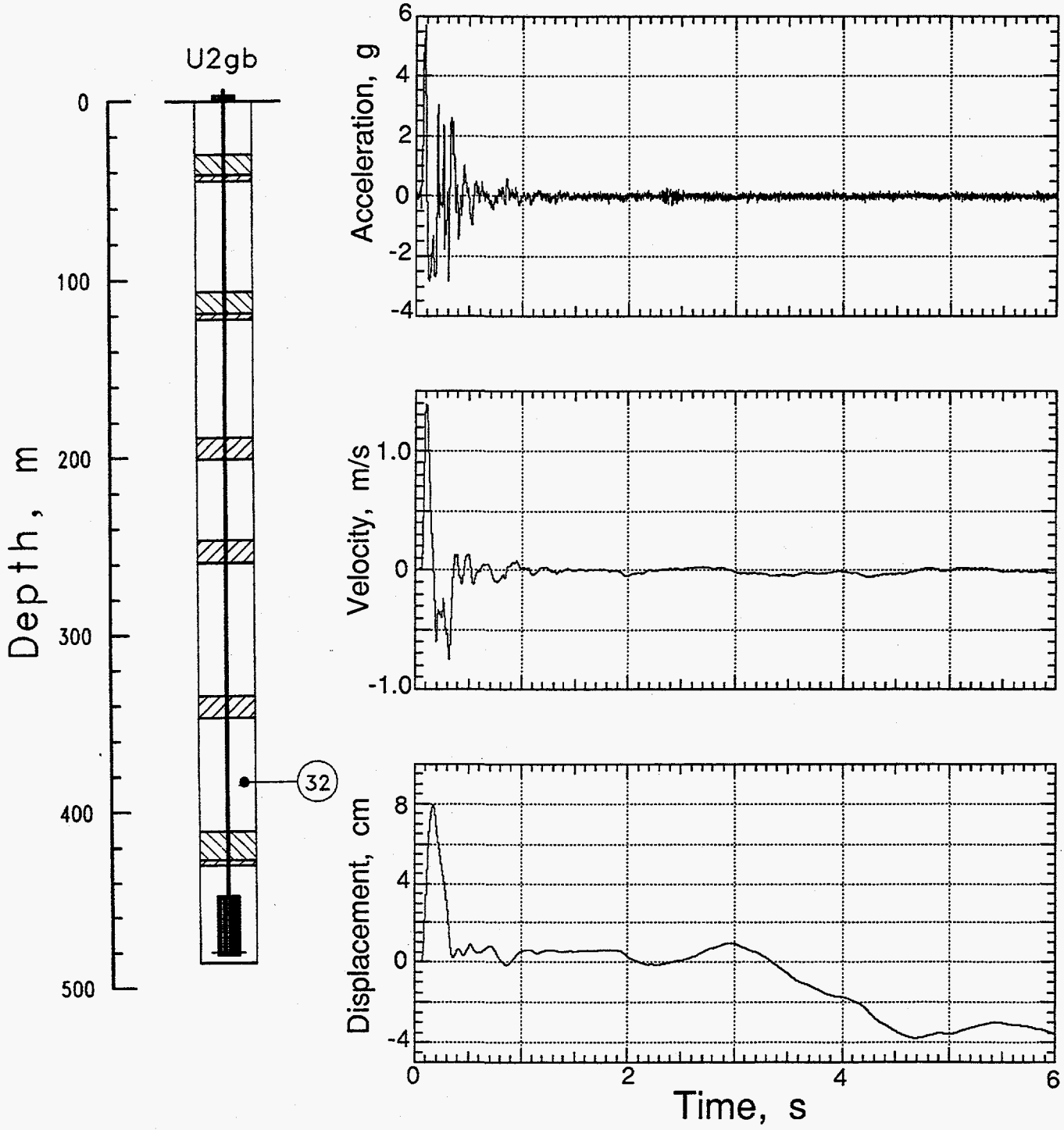

Figure 3.9 Explosion–induced vertical motion in the coarse stemming of the emplacement hole at a depth of 381 m (station 32).

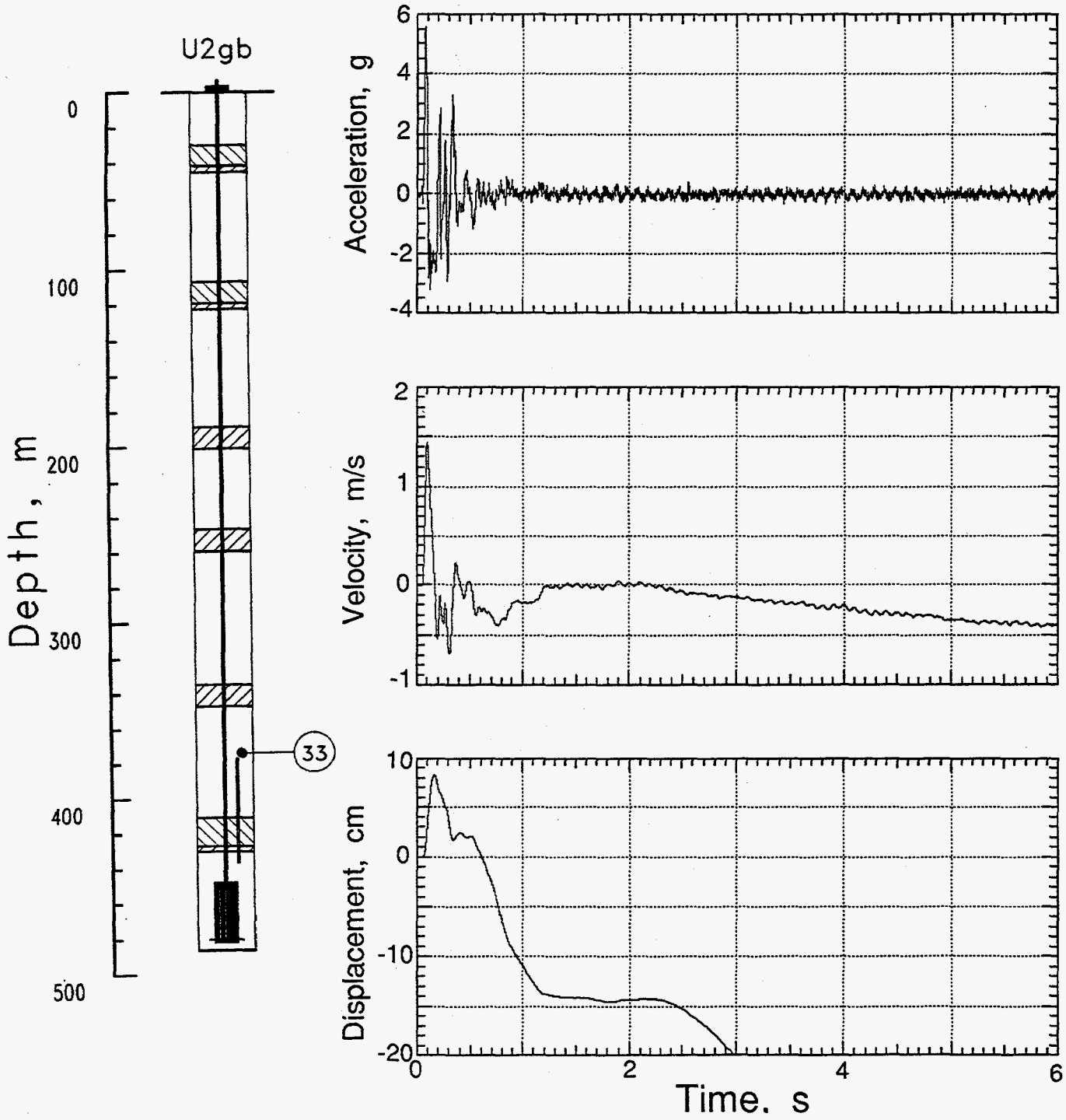

Figure 3.10 Explosion–induced vertical motion in the coarse stemming of the emplacement hole at a depth of 376.1 m (station 33).

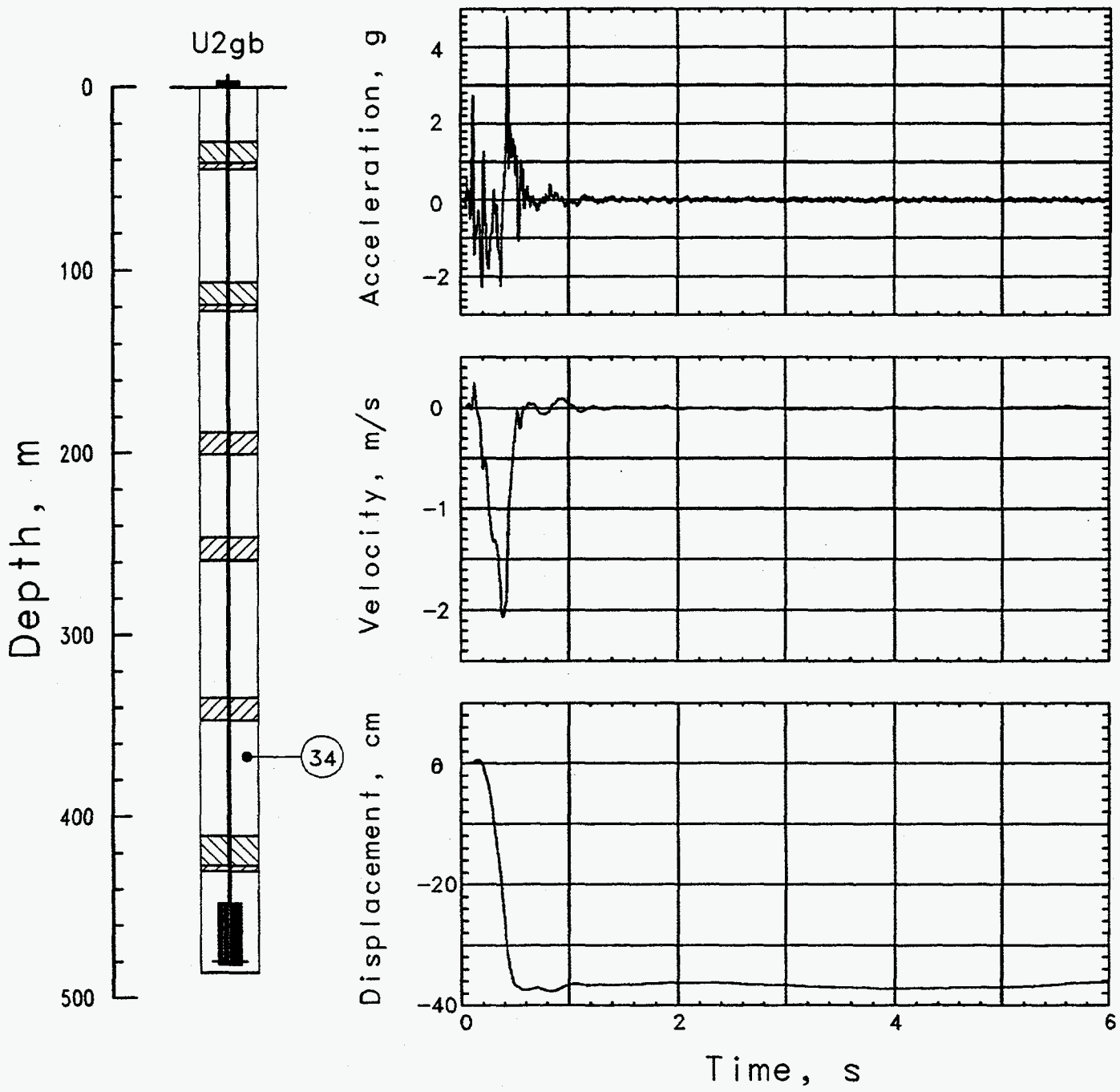

Figure 3.11 Explosion–induced vertical motion in the coarse stemming of the emplacement hole at a depth of 365.8 m (station 34).

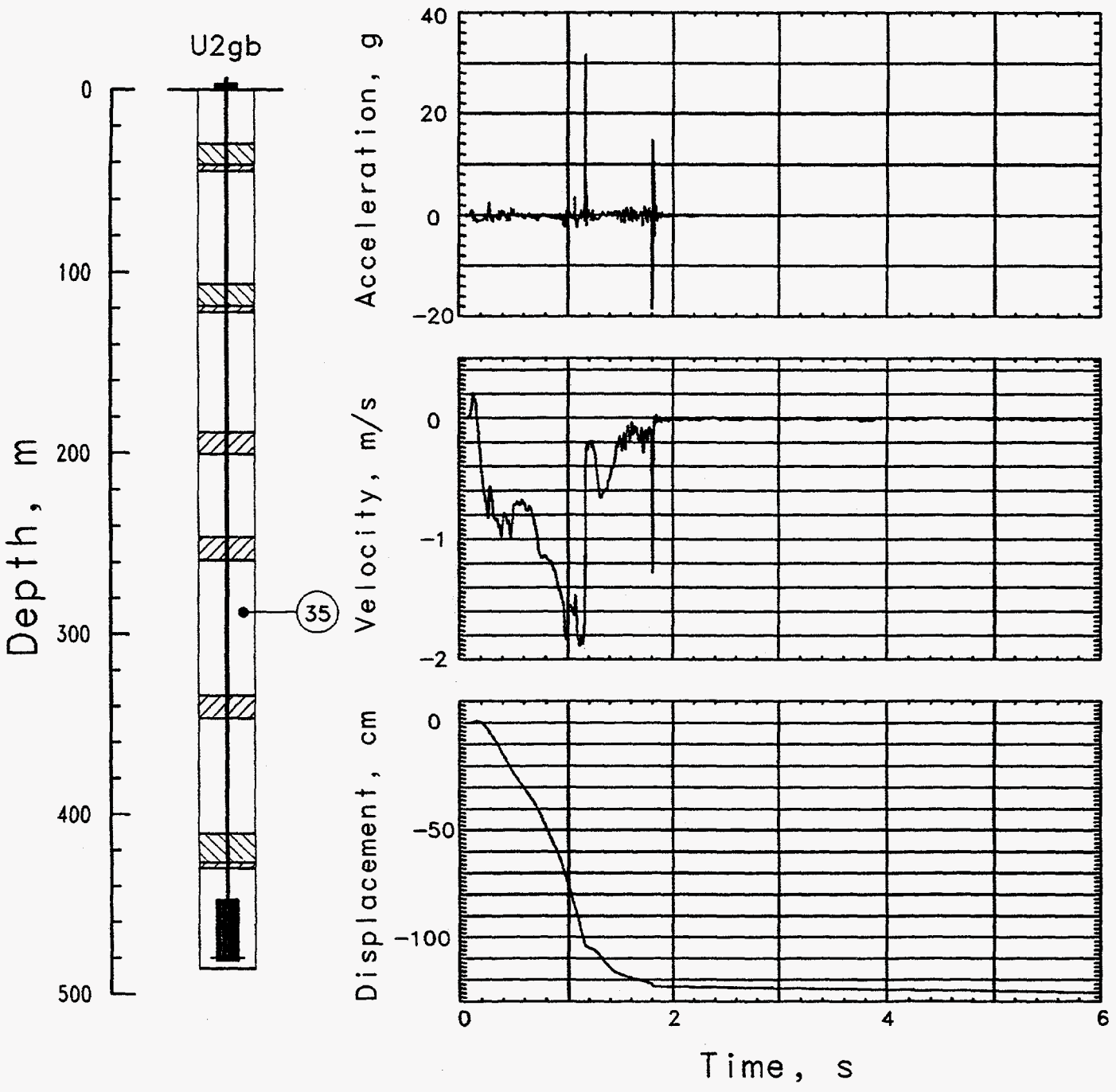

Figure 3.12 Explosion–induced vertical motion in the coarse stemming of the emplacement hole at a depth of 285.1 m (station 35).

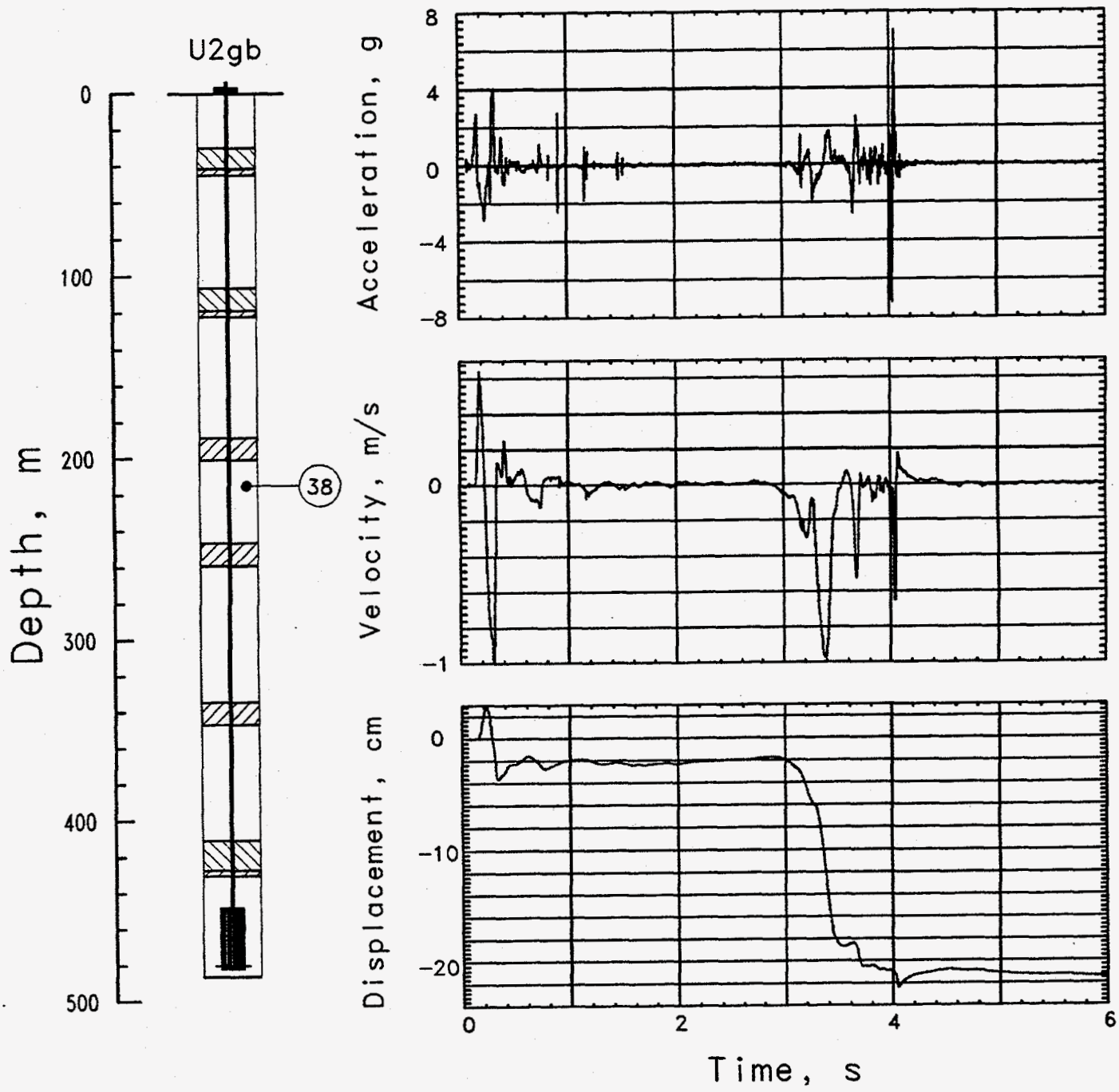

Figure 3.13 Explosion–induced vertical motion in the coarse stemming of the emplacement hole at a depth of 216.5 m (station 38).

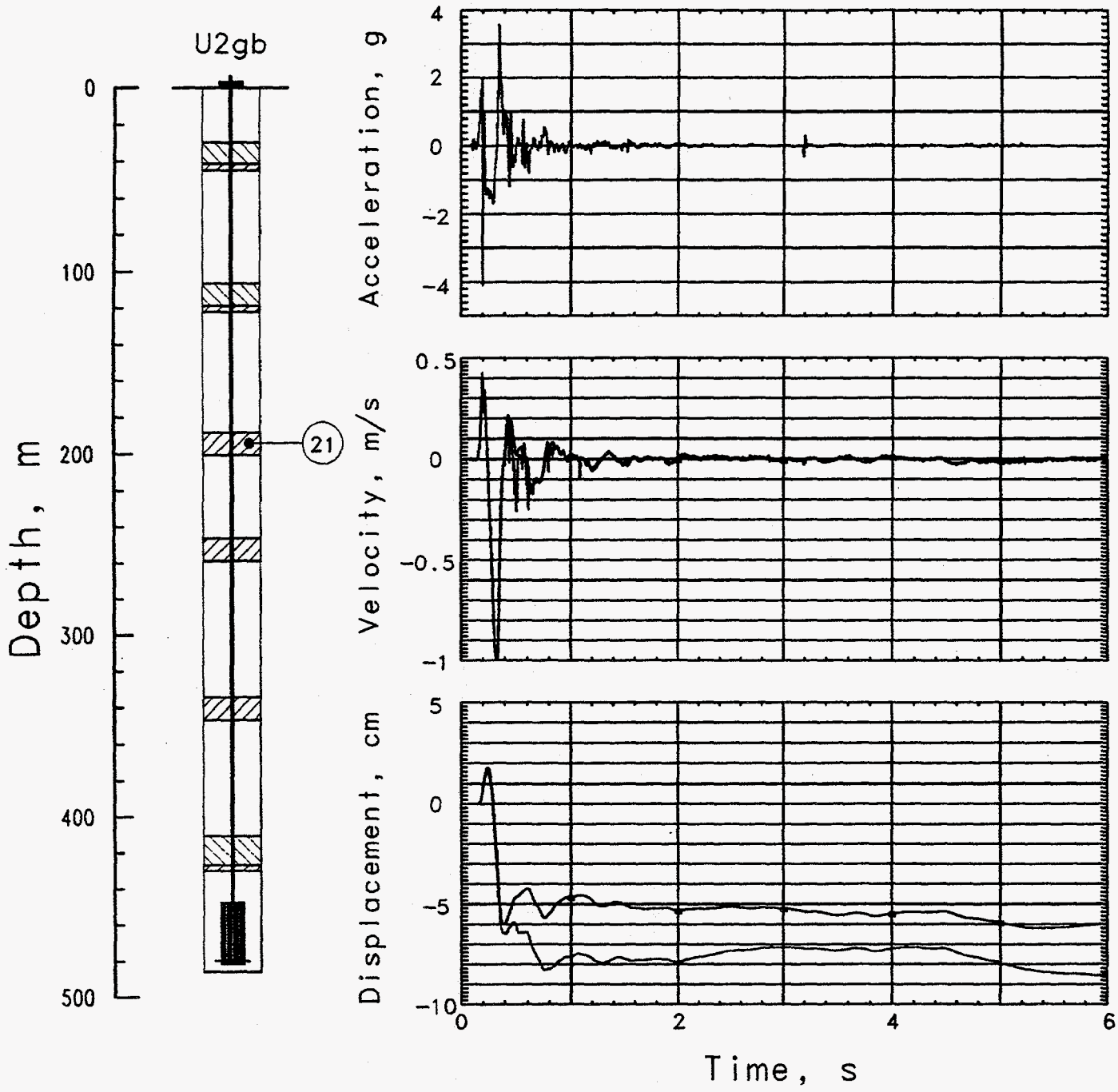

Figure 3.14 Explosion–induced vertical motion in the coarse stemming of the fines plug at a depth of 195.4 m (station 21). Records annotated with an 'a' are derived from the accelerometer.

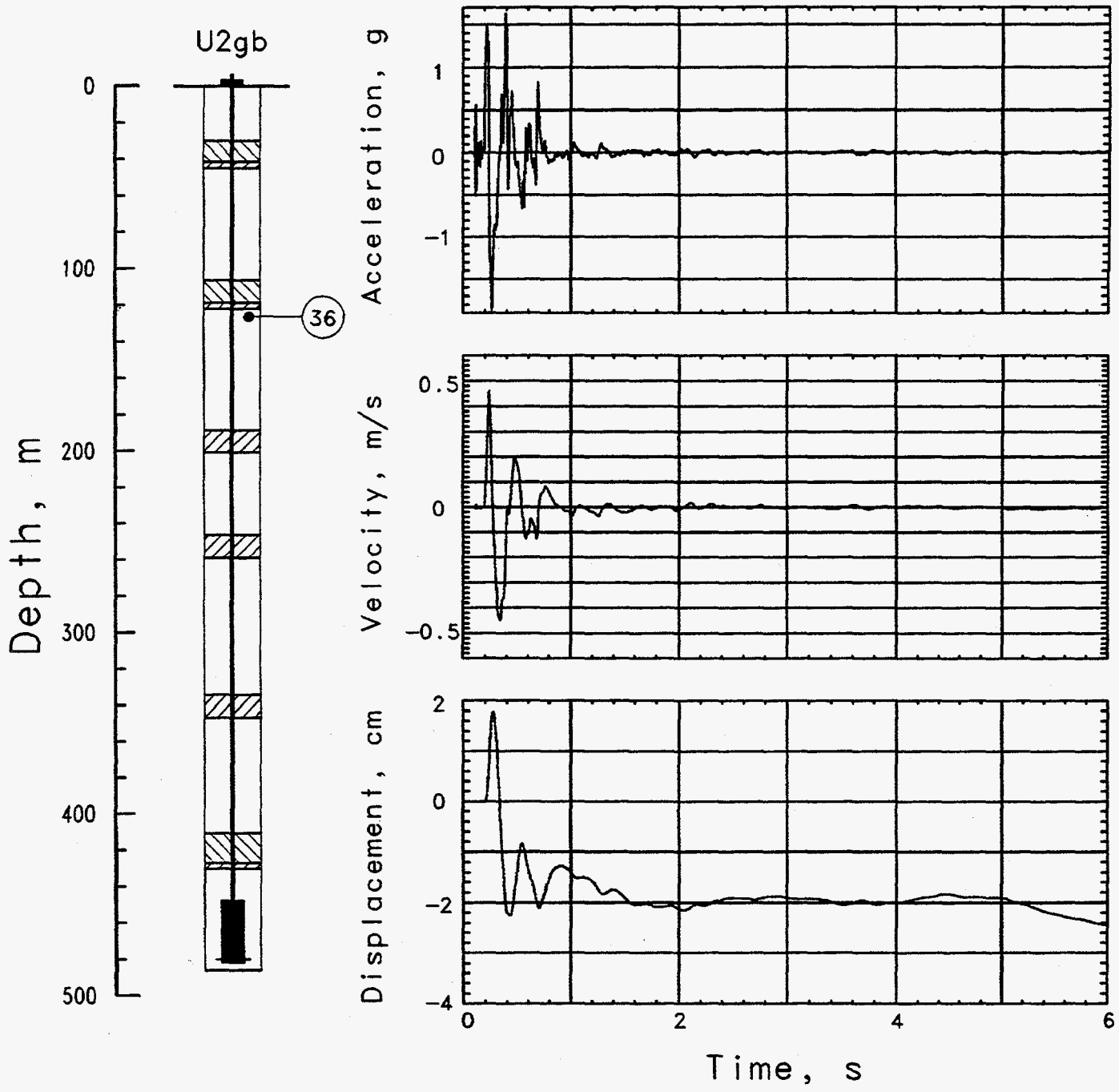

Figure 3.15 Explosion–induced vertical motion in the coarse stemming of the emplacement hole at a depth of 123.4 m (station 36).

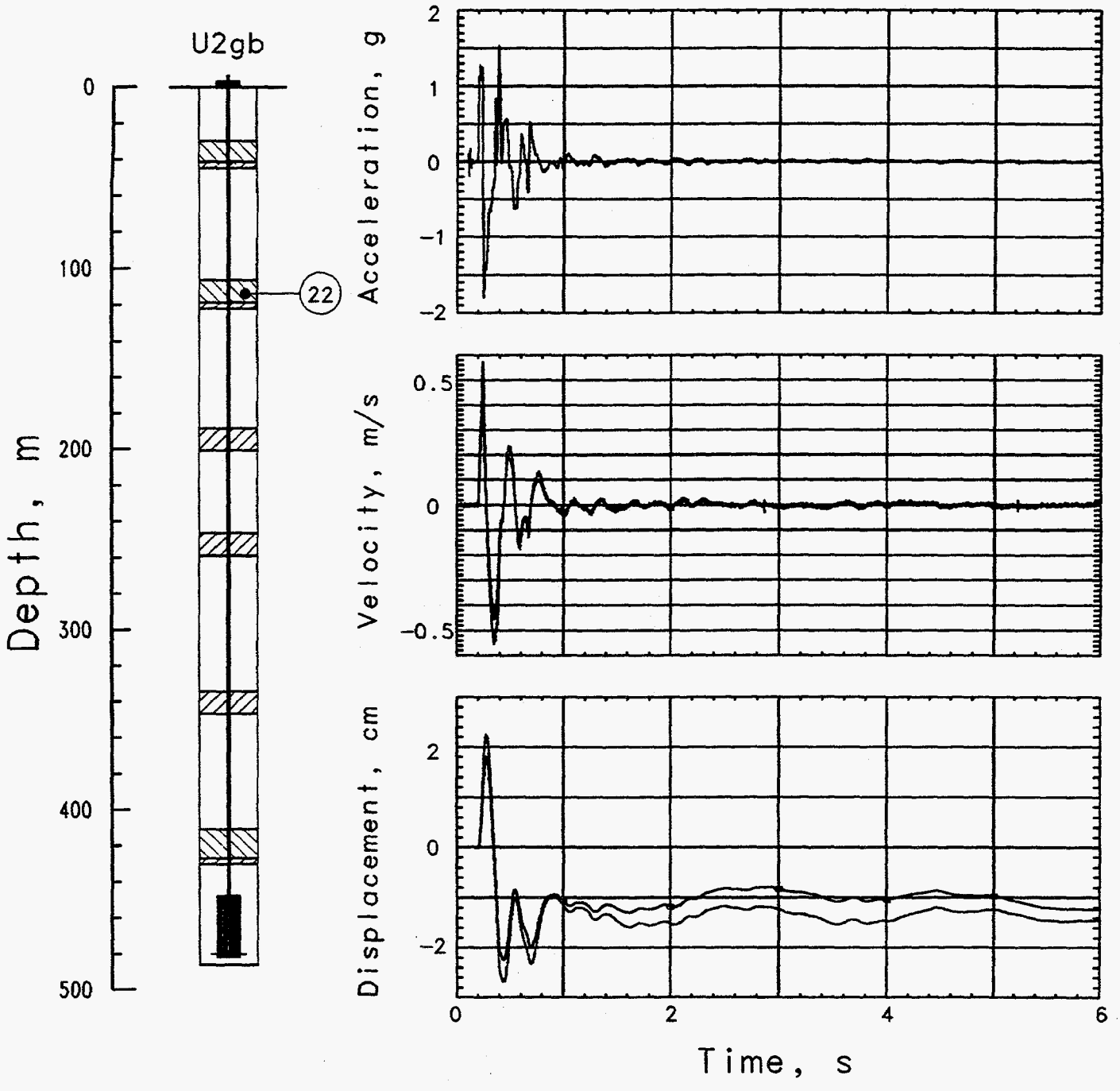

Figure 3.16 Explosion–induced vertical motion in the coarse stemming of the SGC plug at a depth of 113.0 m (station 22). Records annotated with an 'a' are derived from the accelerometer.

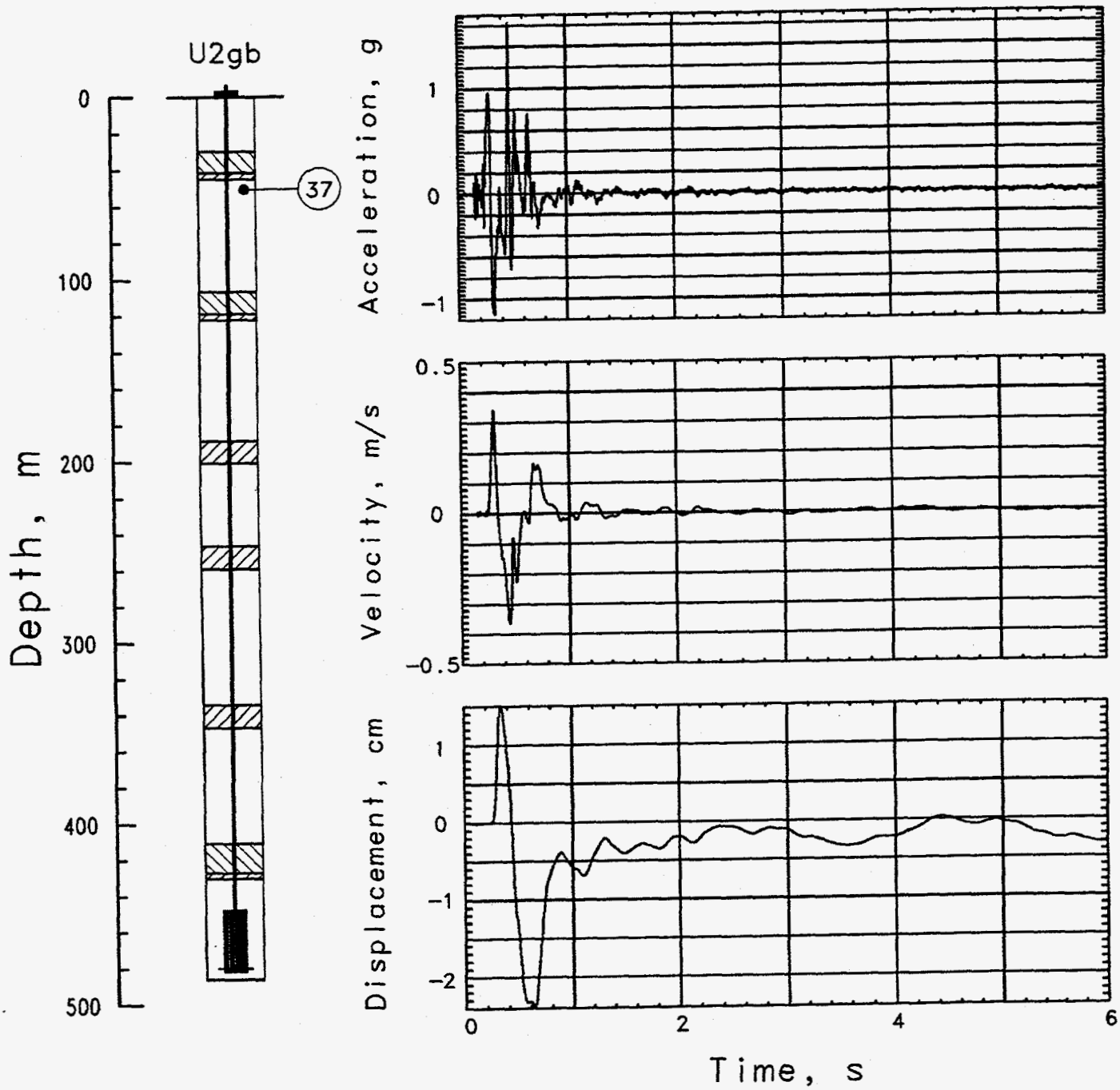

Figure 3.17 Explosion–induced vertical motion in the coarse stemming of the emplacement hole at a depth of 46.8 m (station 37).

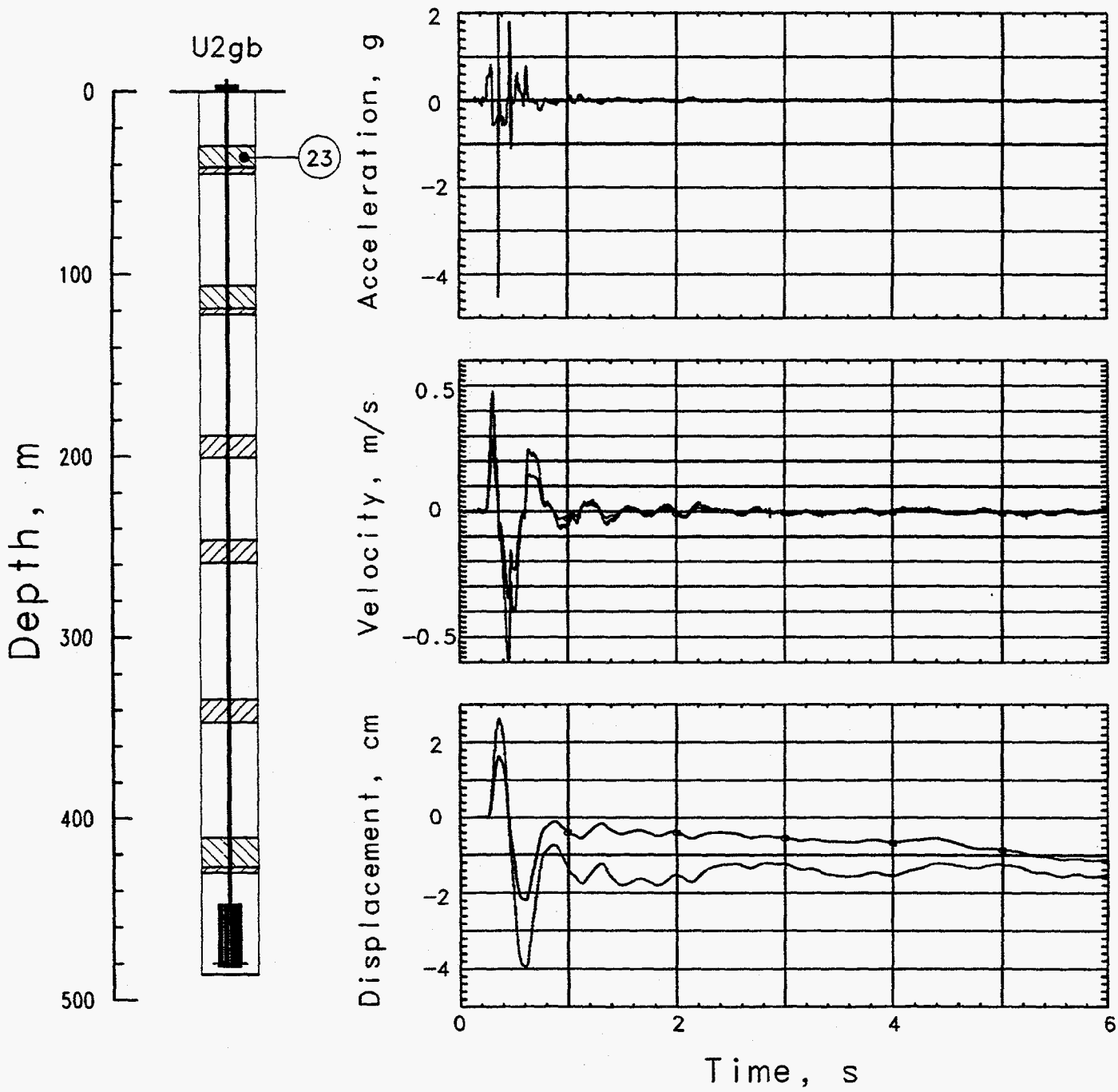

Figure 3.18 Explosion–induced vertical motion in the coarse stemming of the SGC plug at a depth of 36.0 m (station 23). Records annotated with an 'a' are derived from the accelerometer.

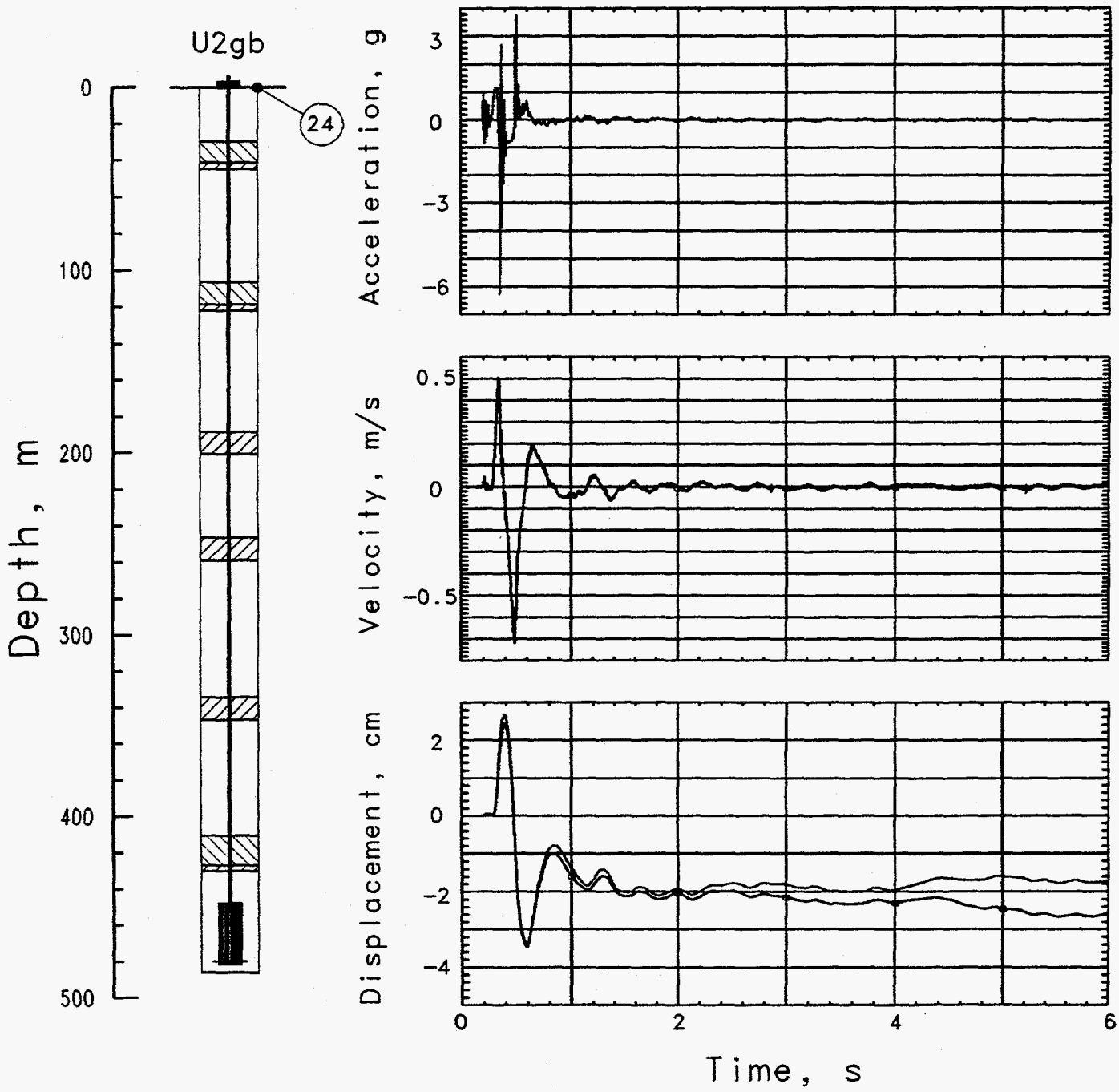

Figure 3.19 Explosion–induced vertical motion of the surface casing (station 24). Records annotated with an 'a' are derived from the accelerometer.

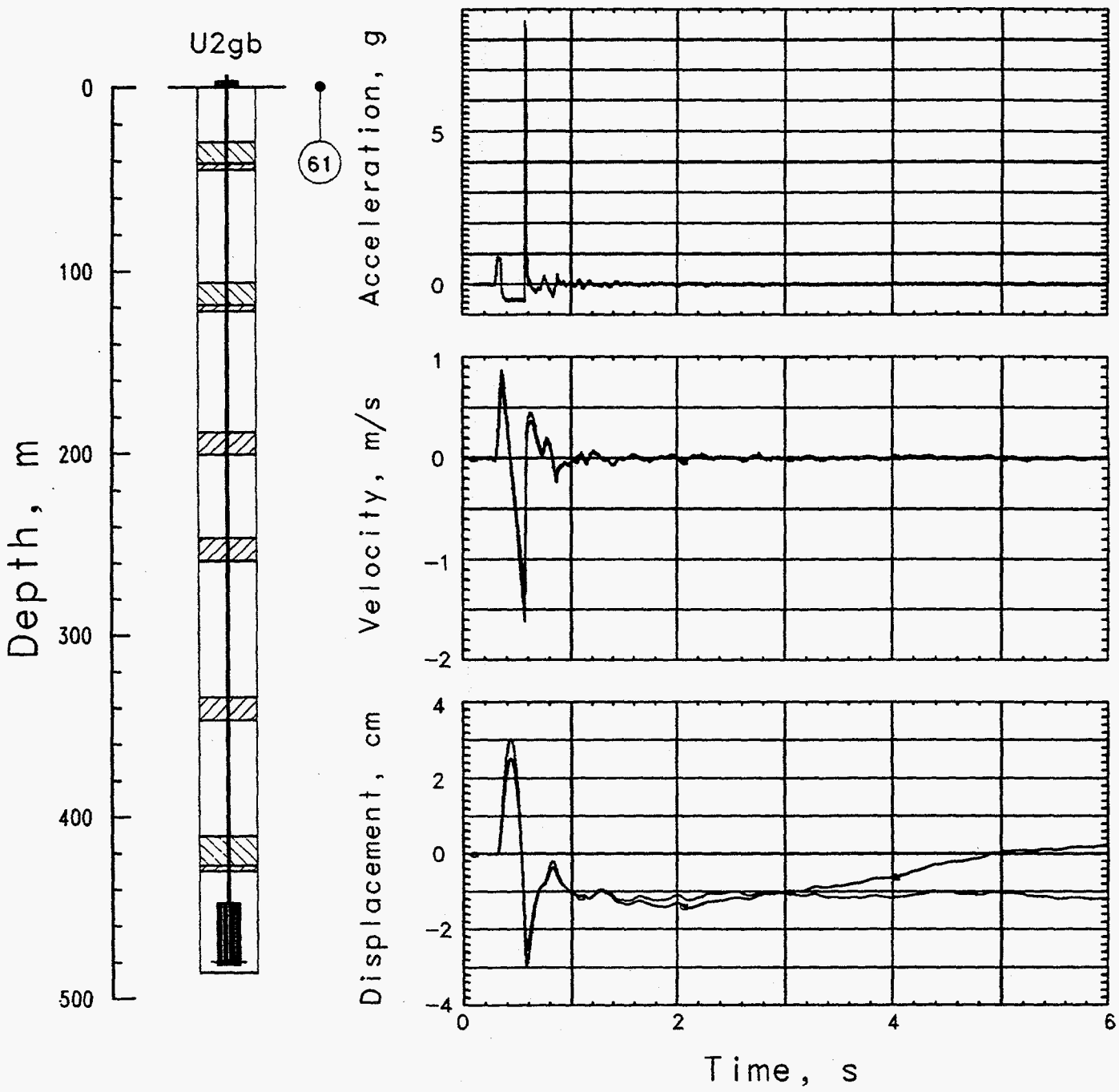

Figure 3.20 Explosion–induced vertical motion in the ground surface at a depth of 0.91 m and a horizontal distance of 15.24 m from Surface Ground Zero (station 61). Records annotated with an 'a' are derived from the accelerometer.

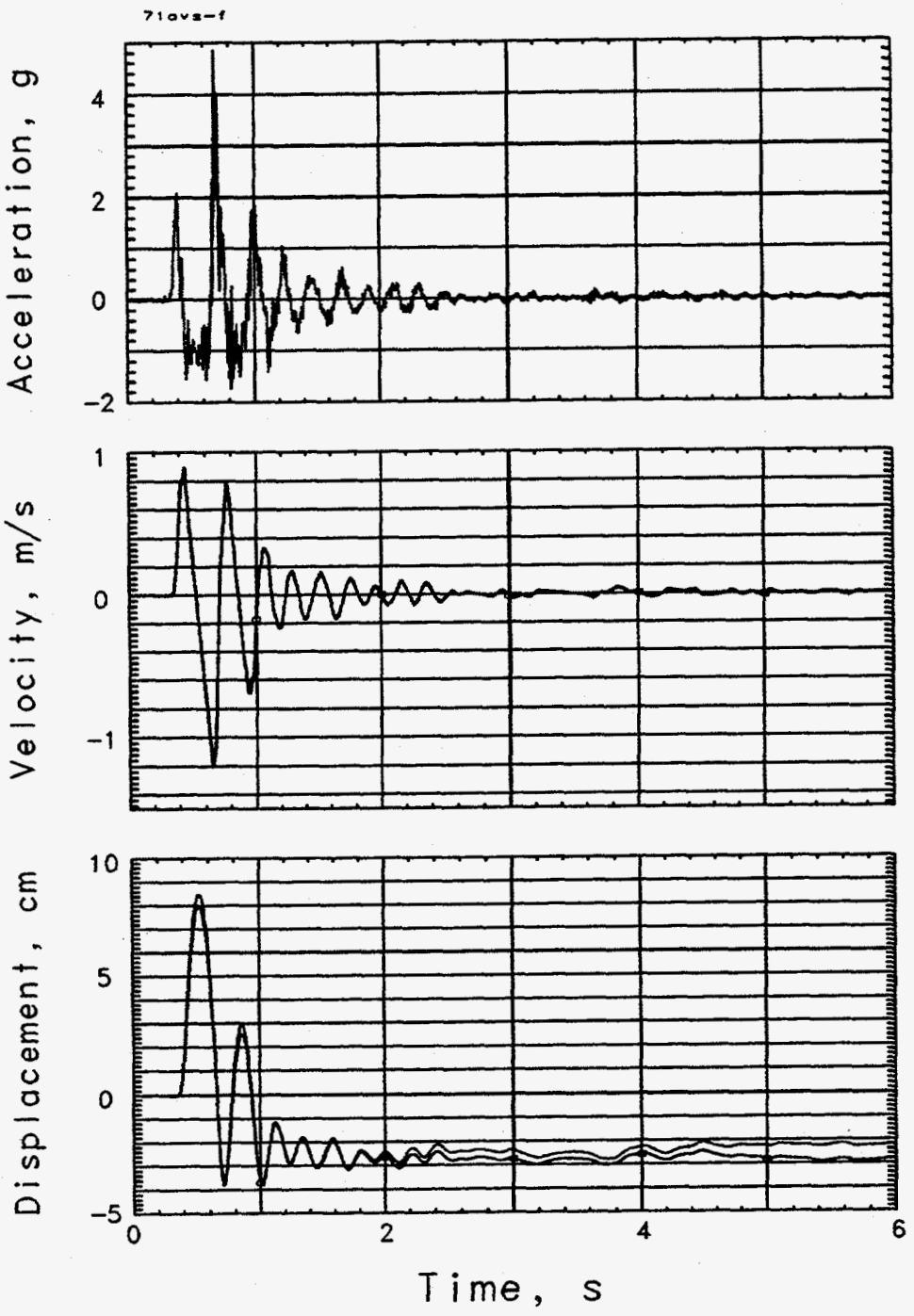

Figure 3.21 Explosion–induced vertical motion of the recording trailer (station 71). Records annotated with an 'a' are derived from the accelerometer.

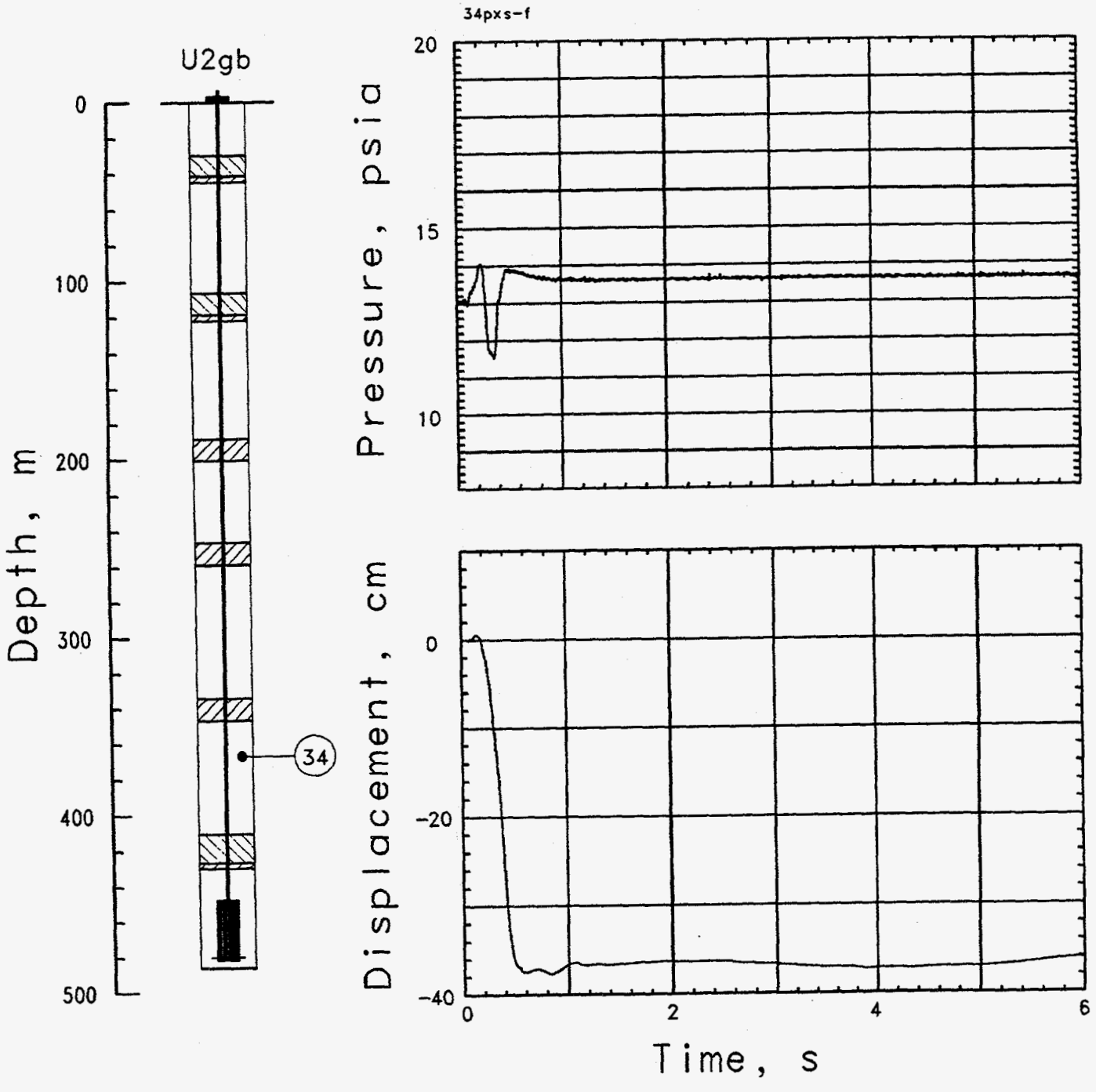

Figure 3.22 Comparison of the first six seconds of explosion–induced displacement with gas pressure measured below the deepest fines plug (station 34).

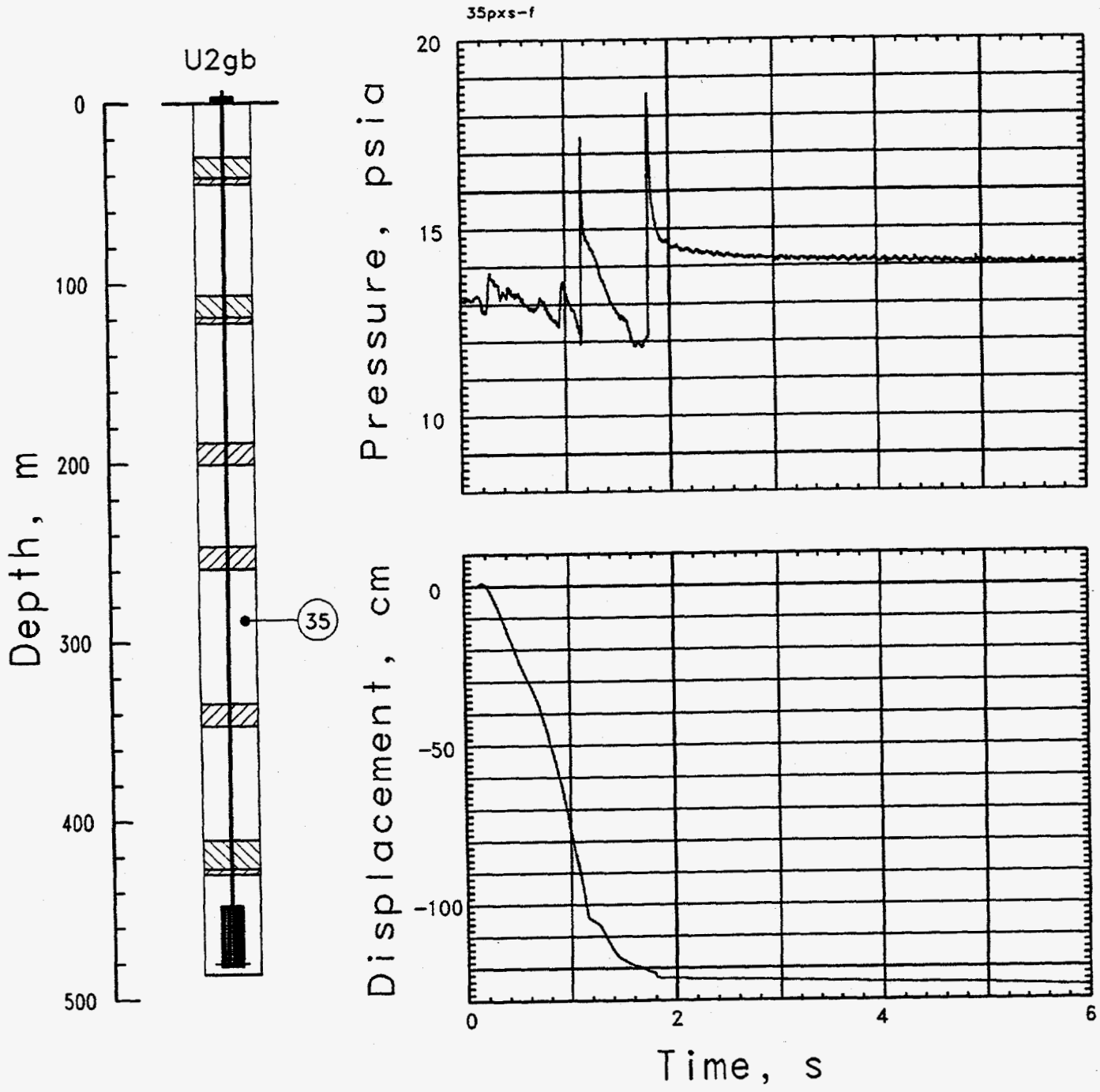

Figure 3.23 Comparison of the first six seconds of explosion–induced displacement with gas pressure measured below the second fines plug (station 35).

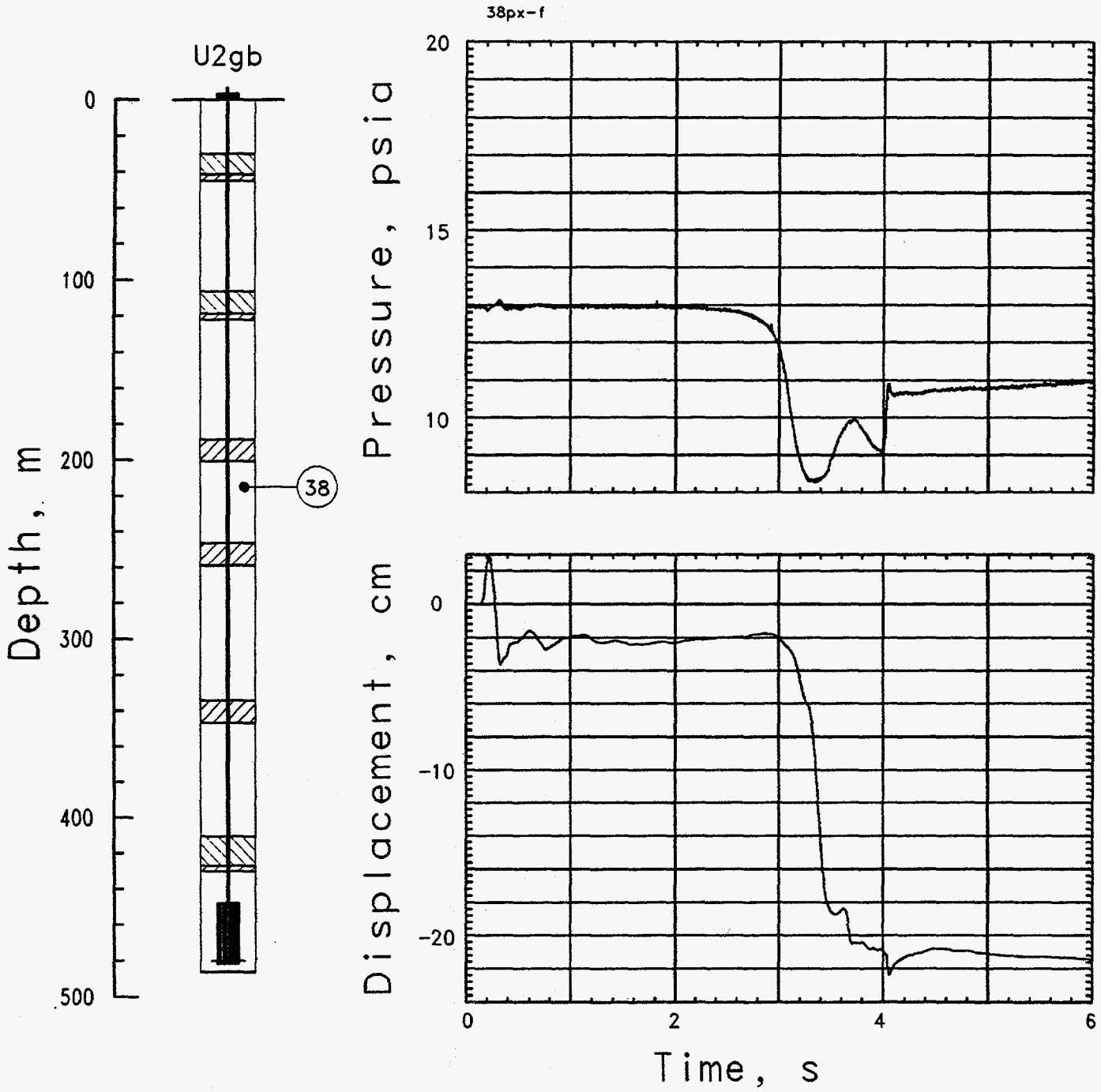

Figure 3.24 Comparison of the first six seconds of explosion–induced displacement with gas pressure measured below the third fines plug (station 38).

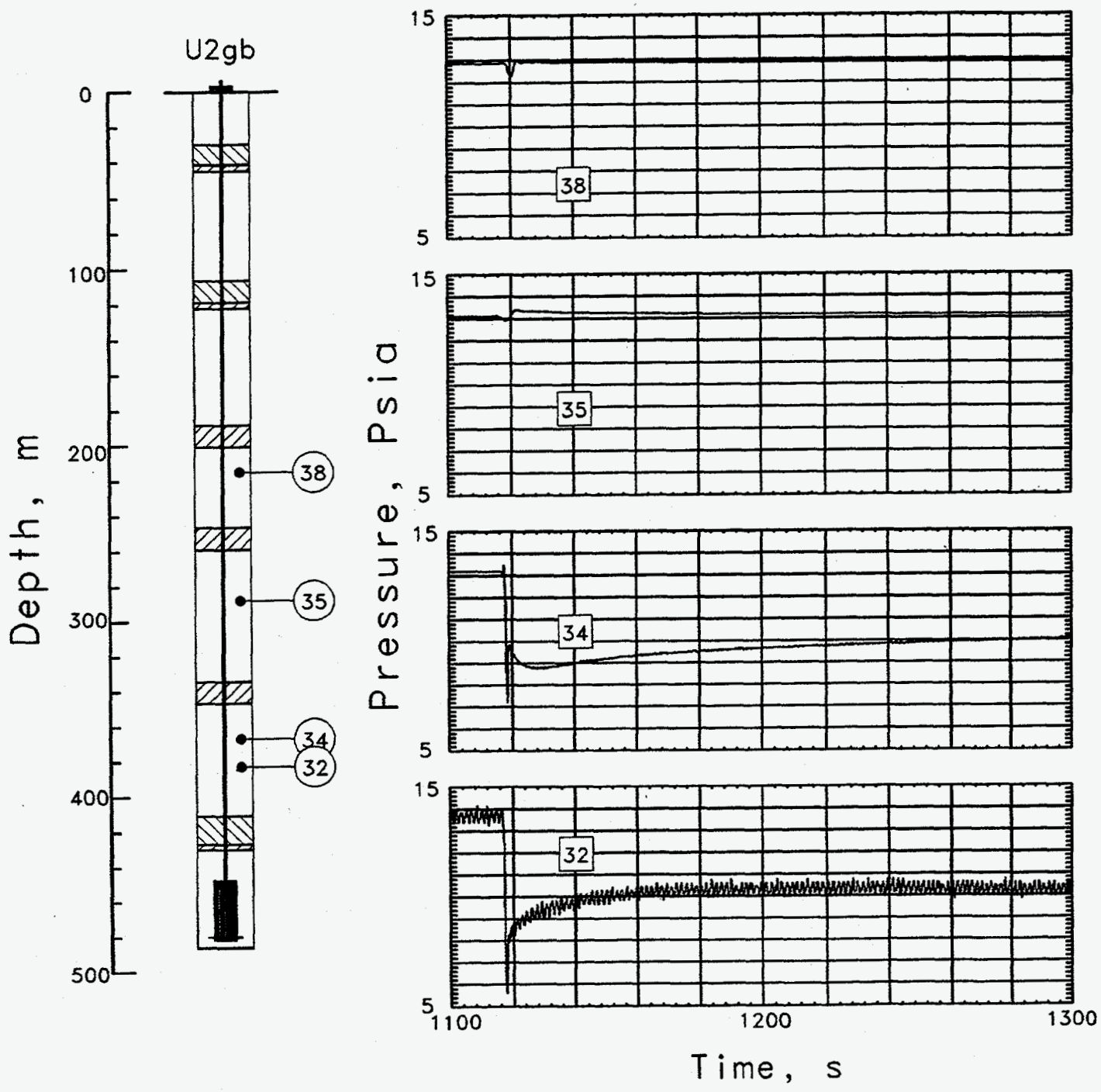

Figure 3.25 Pressures measured in the stemming column during the collapse episode. The data from station 32 were left unfiltered to expose the full time resolution of the measured signal.

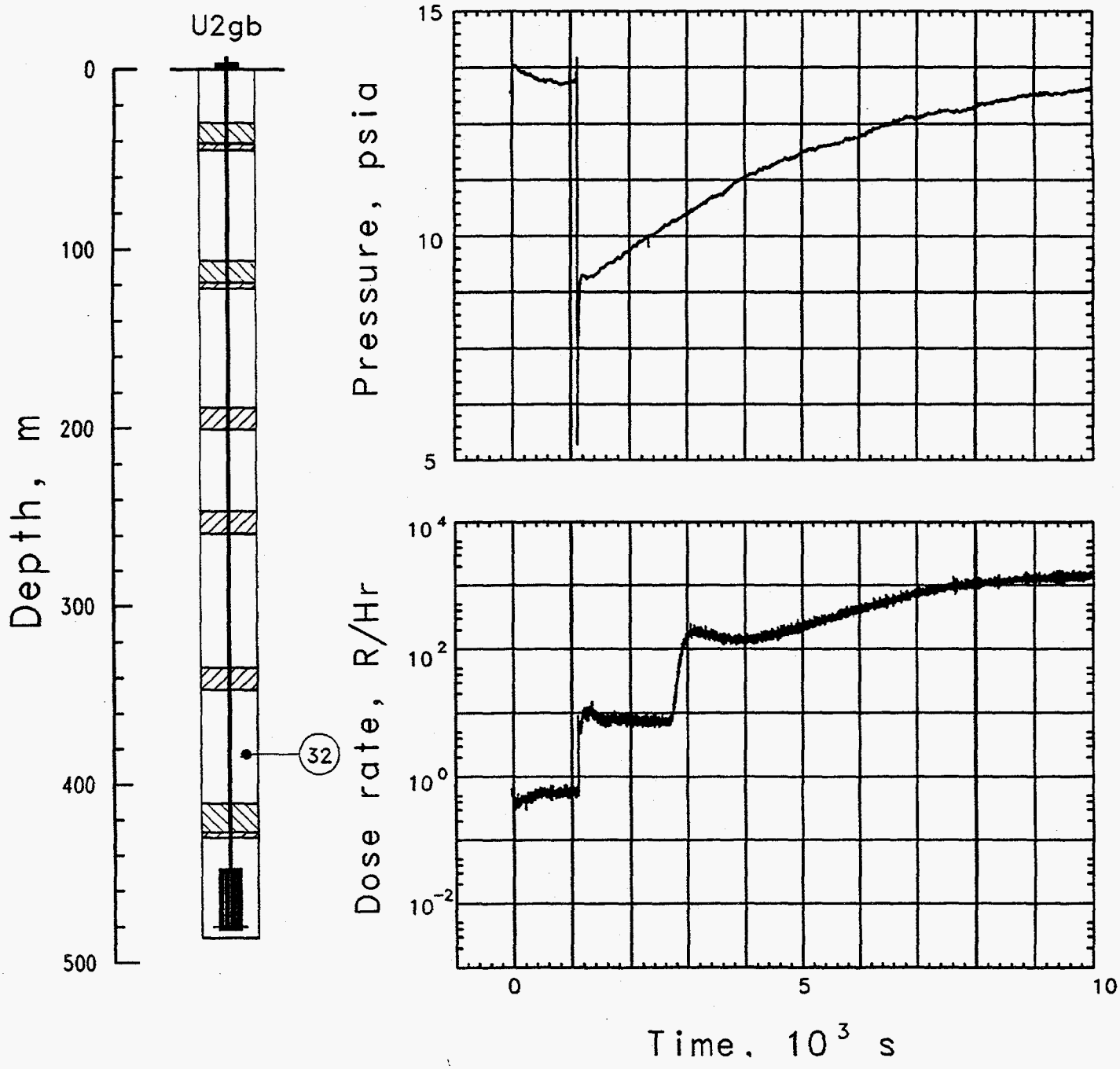

Figure 3.26 Pressure and radiation wave forms for the first 10,000 s after detonation. A first radiation arrival at collapse (1118 s) is evident, with a second arrival at about 2700 seconds. This second arrival may be due to a stemming rearrangement, not seen in the pressure wave form.

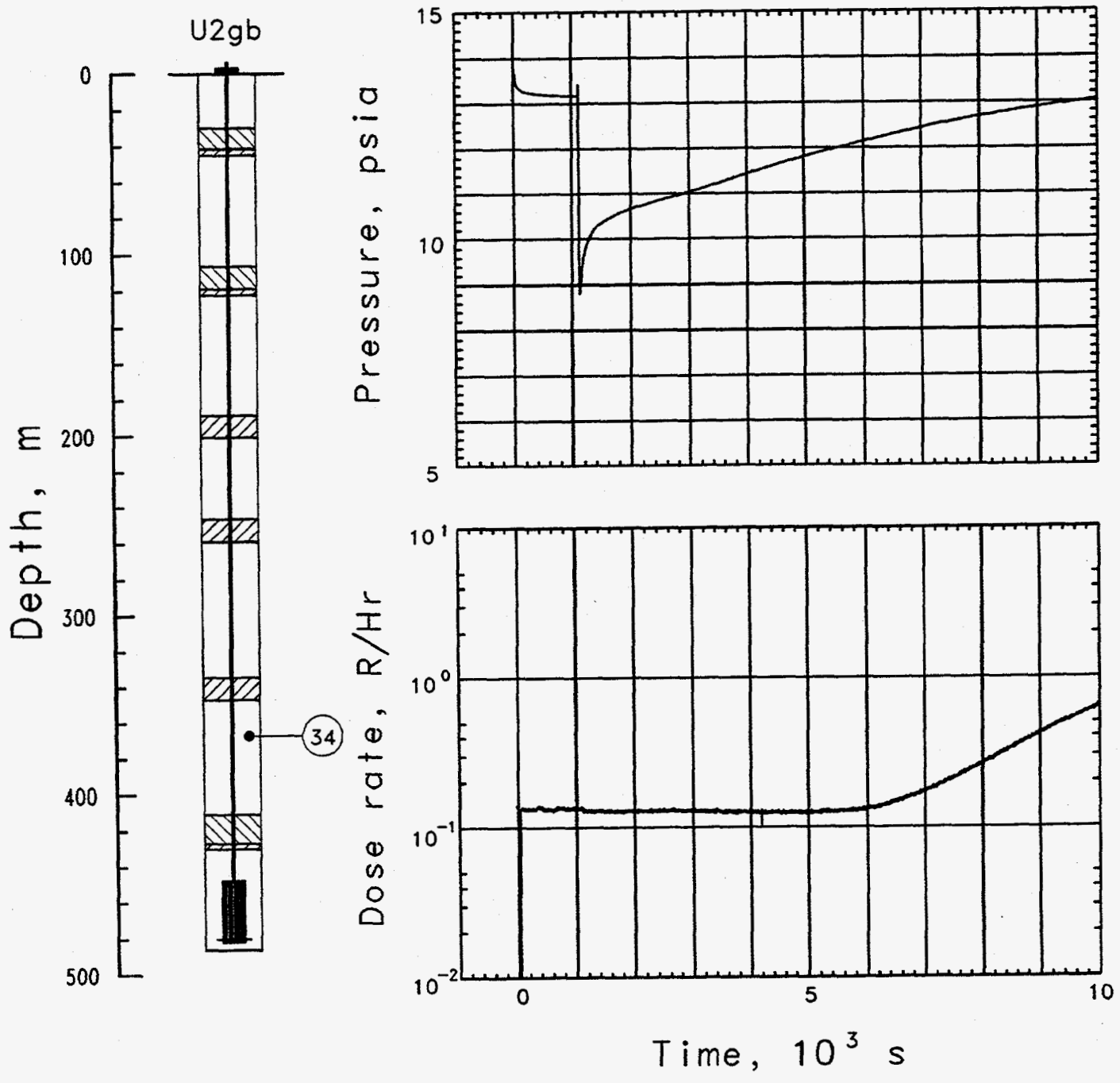

Figure 3.27 Pressure and radiation wave forms for the first 10,000 s after detonation. Radiation arrives at about 5400 s, more than one hour after the collapse.

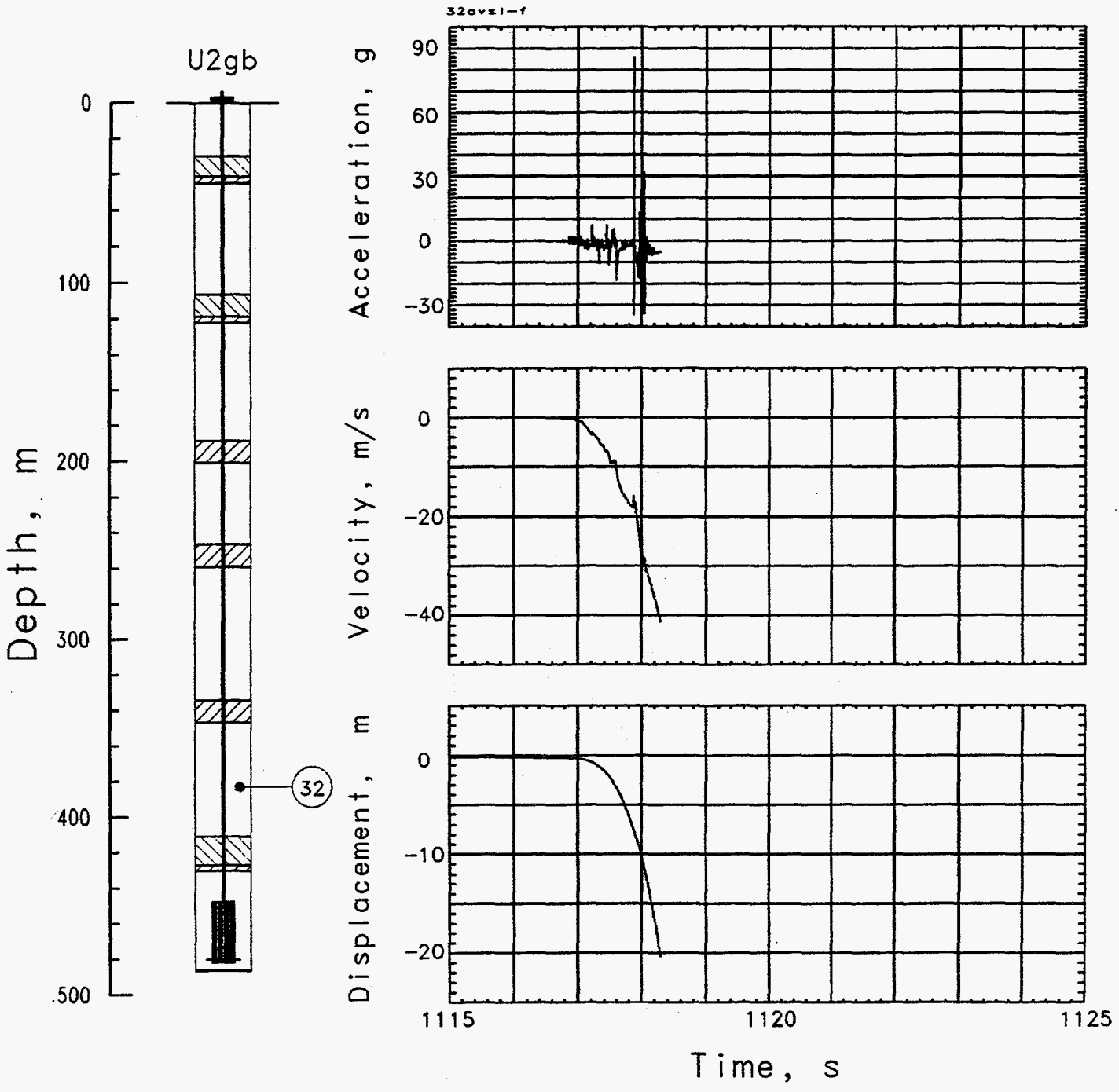

Figure 3.28 Collapse–induced vertical motion in the coarse stemming of the emplacement hole at a depth of 381 m (station 32). Motion signals from this station were terminated at about 1118 s.

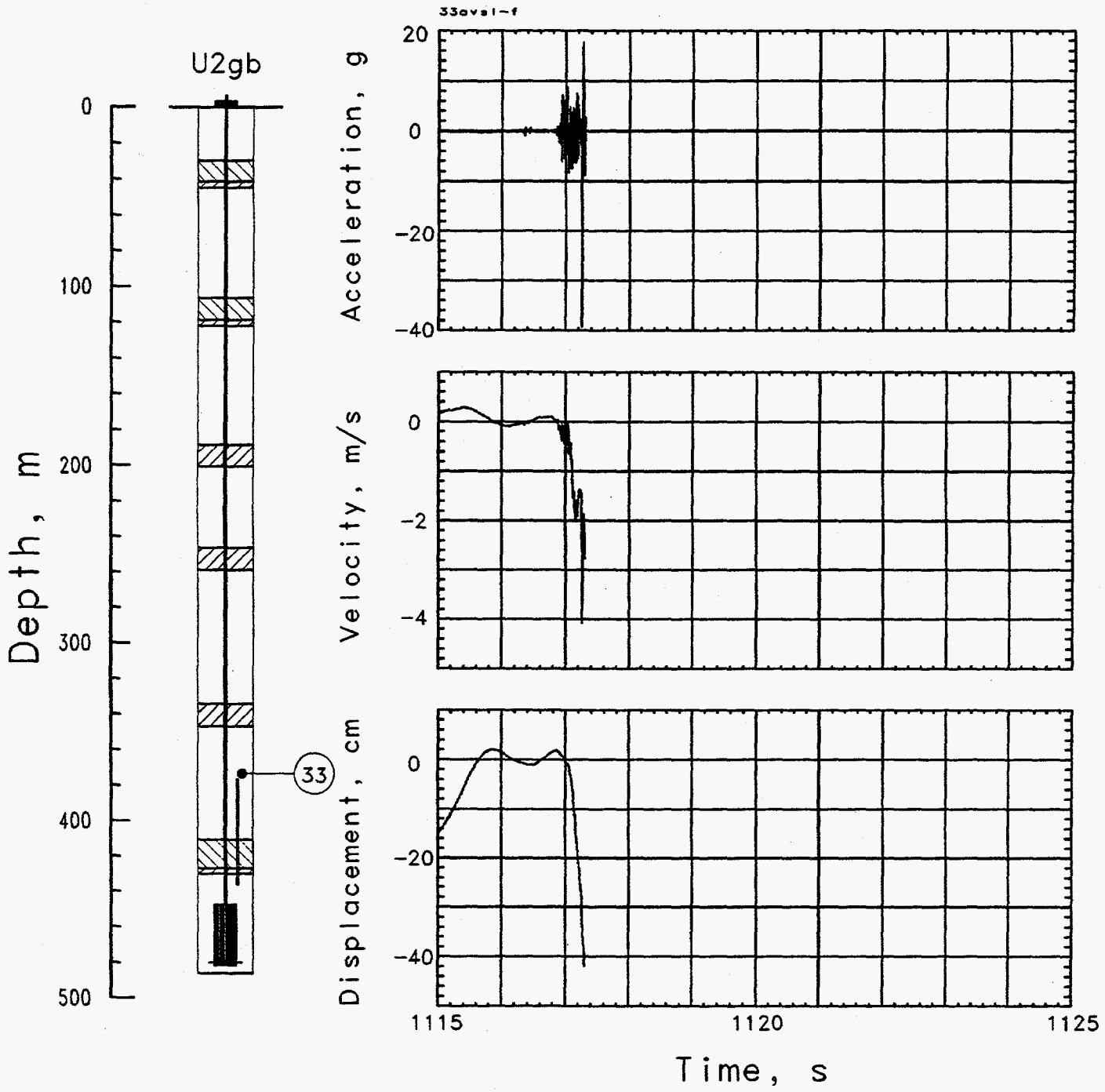

Figure 3.29 Collapse–induced vertical motion in the coarse stemming of the emplacement hole at a depth of 375.1 m (station 33). Motion signals from this station were terminated at about 1117 s.

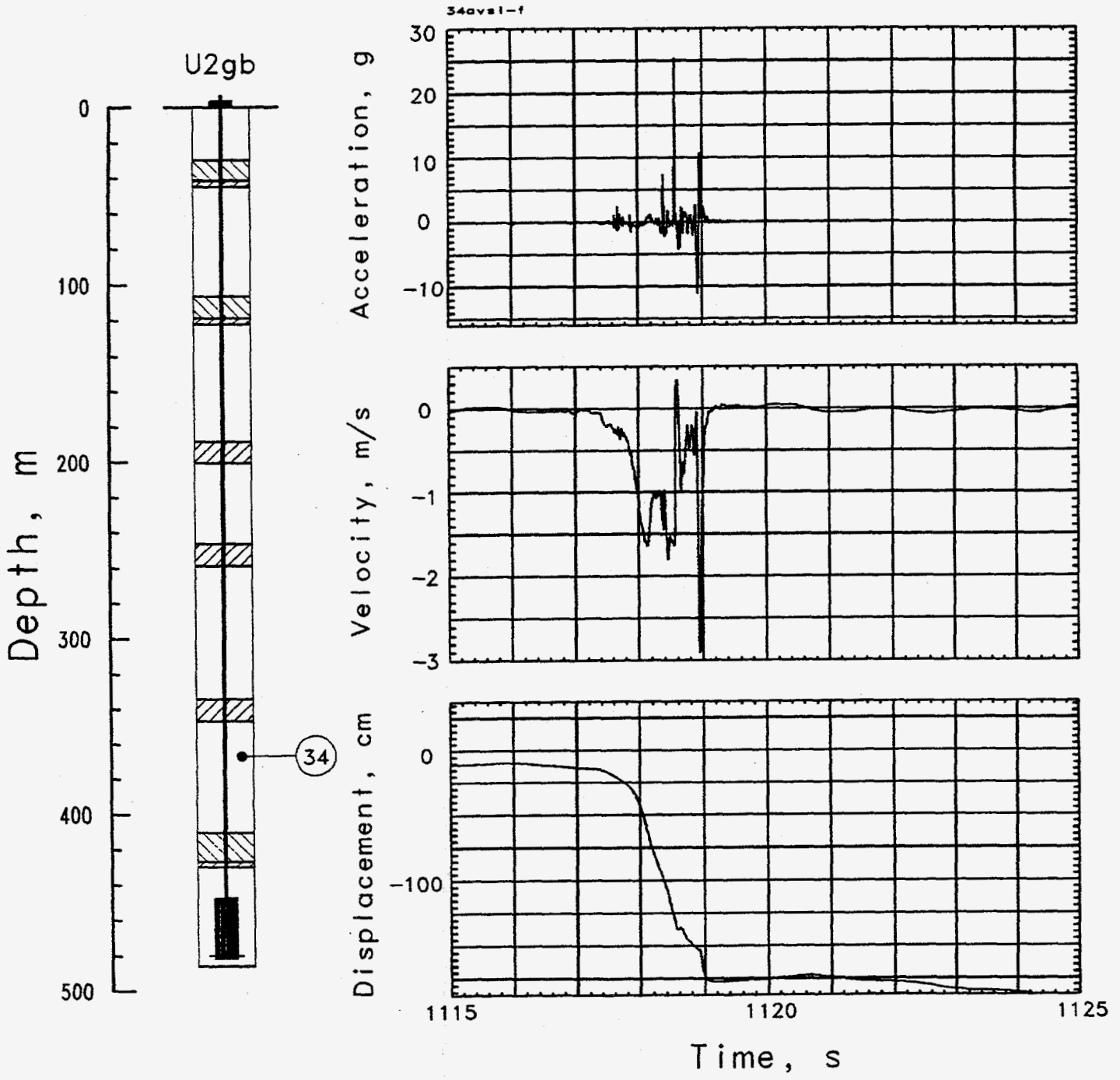

Figure 3.30 Collapse–induced vertical motion in the coarse stemming of the emplacement hole at a depth of 365.7 m (station 34).

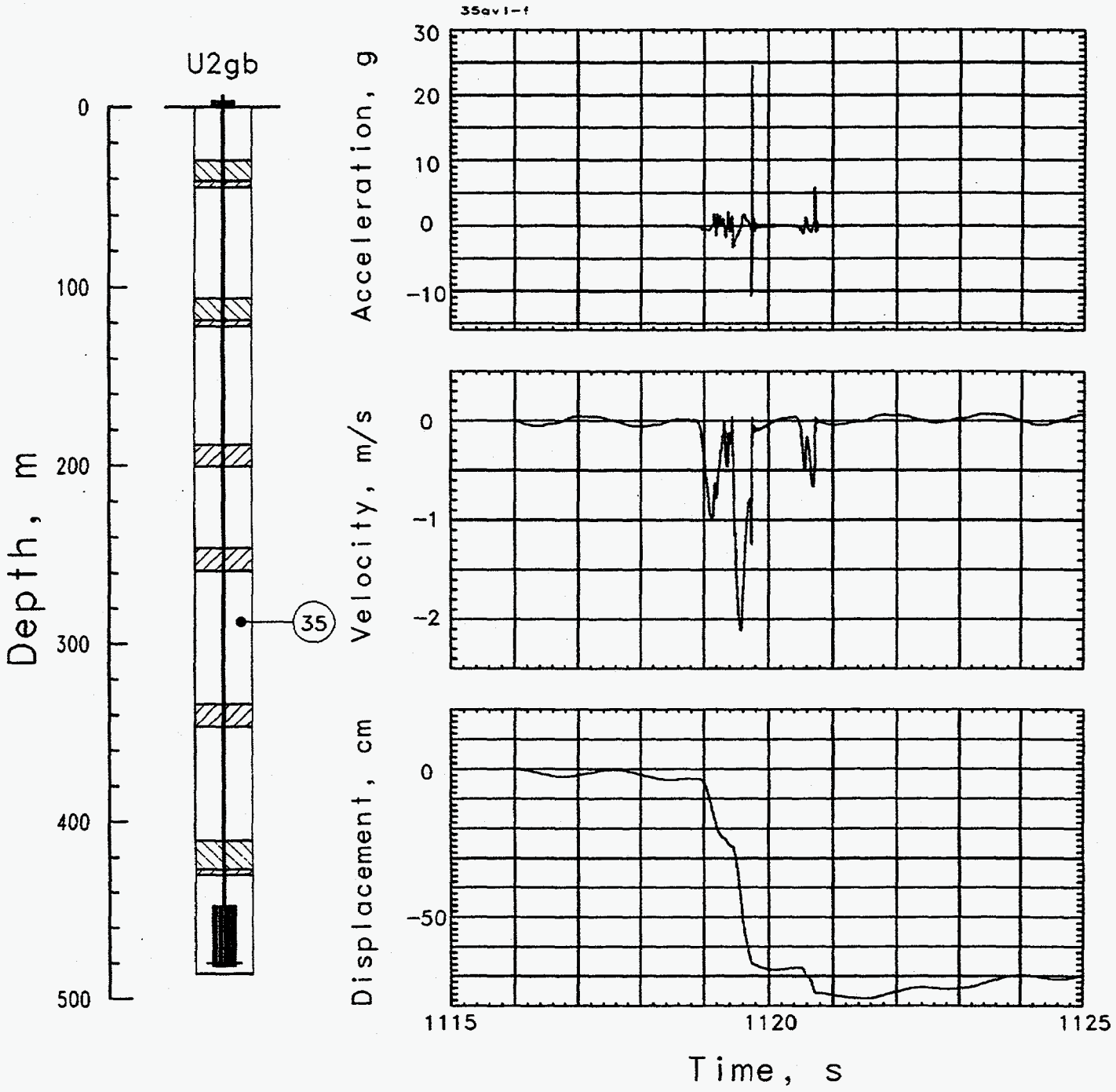

Figure 3.31 Collapse–induced vertical motion in the coarse stemming of the emplacement hole at a depth of 285.1 m (station 35).

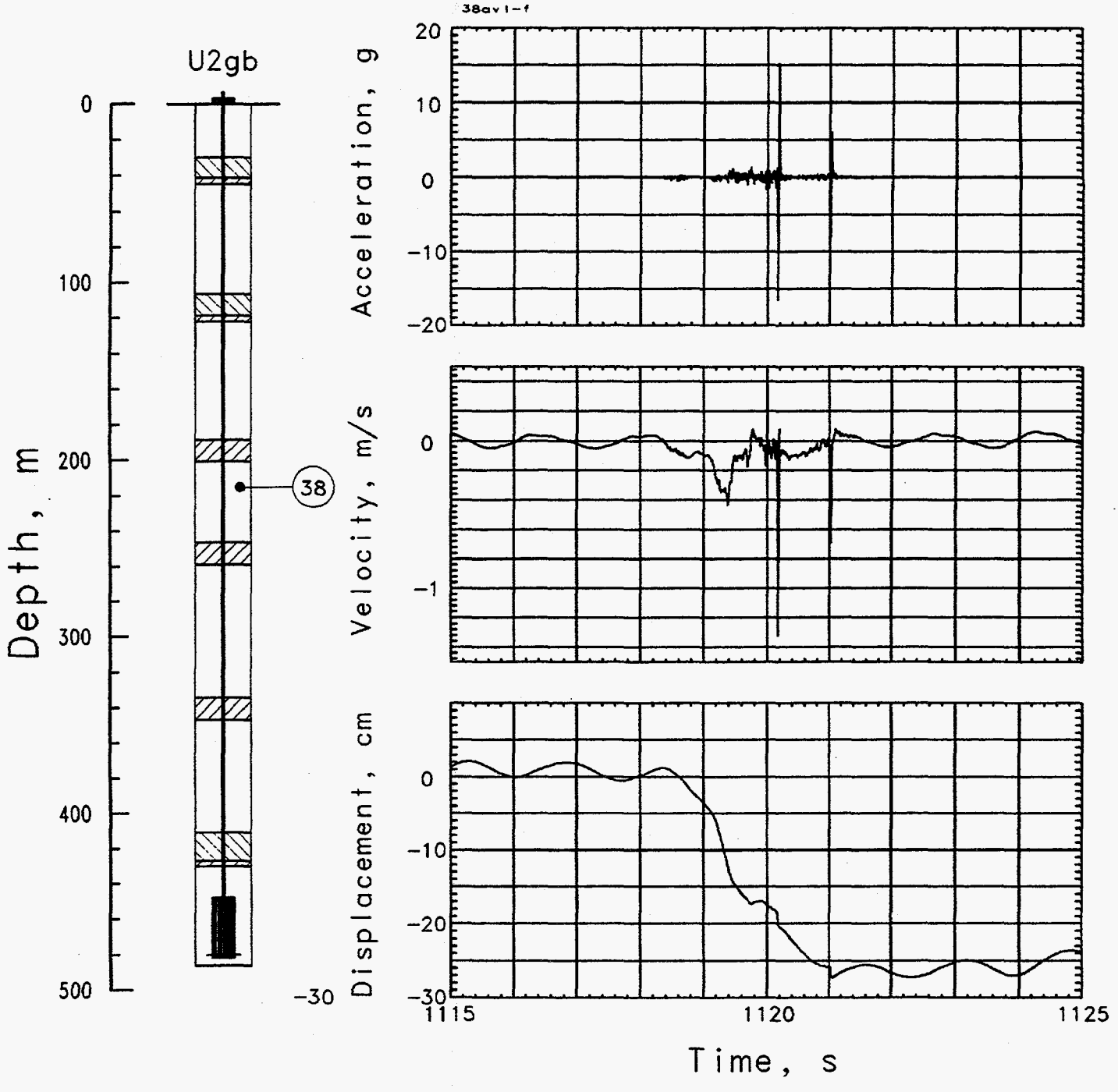

Figure 3.32 Collapse–induced vertical motion in the coarse stemming of the emplacement hole at a depth of 216.5 m (station 38).

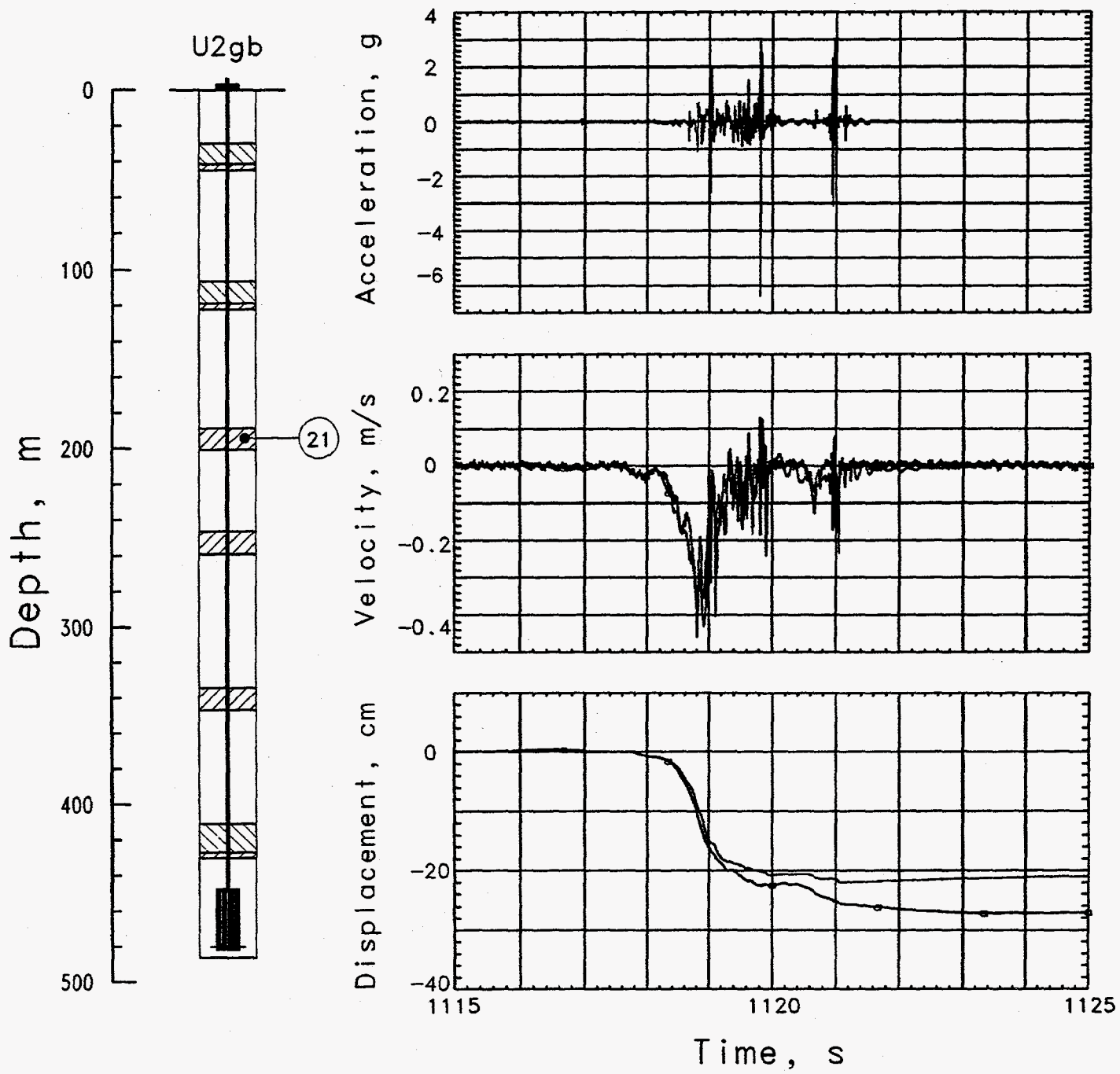

Figure 3.33 Collapse–induced vertical motion in the fines plug at a depth of 195.4 m (station 21). Records annotated with an 'a' are derived from the accelerometer.

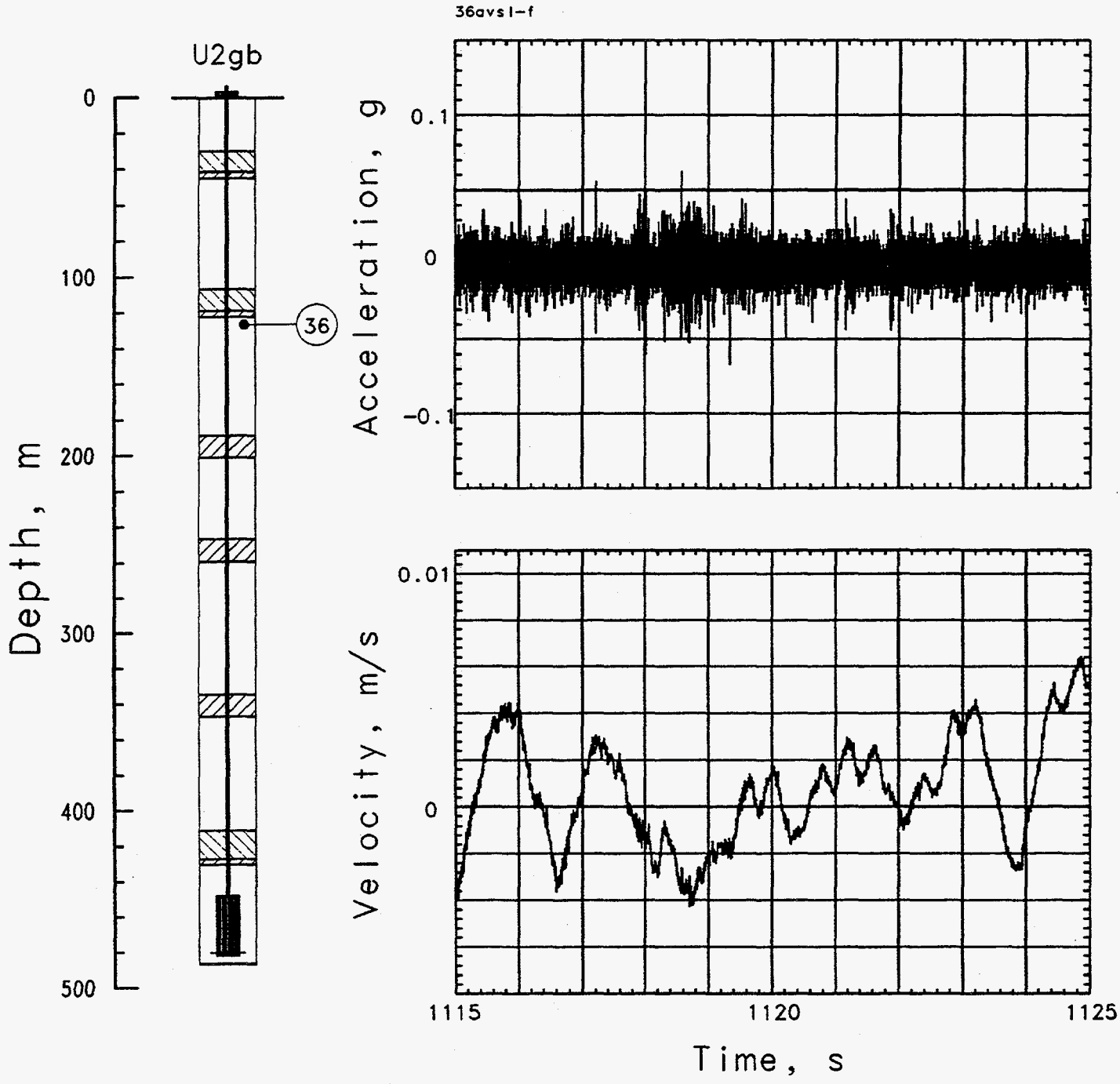

Figure 3.34 Vertical motion in the coarse stemming of the emplacement hole at a depth of 123.4 m (station 36) during the time of collapse. Collapse signals were not sensed at or above this station.

4 Other Measurements

4.1 Geophone station in the trailer park

Figures 4.1 shows the data as recorded on a high sensitivity accelerometer and a geophone mounted in the ground surface of the trailer park (station 62).

4.2 Gas sample hose

Figure 4.2 shows the displacement of the gas sample hose as measured by a rotary potentiometer mounted between the gas sample skid and the hose (station 39). This device has a full displacement range of 22.9 m and had an initial offset of about 4 m.

4.3 Stress in the bottom plug

Biaxial stress and strain transducers[4] were mounted at two elevations in the bottom SGC plug. The active elements for stress were Ytterbium while the strain elements were composed of Constantan. Orientation of the station 1 was is if strain were a vector quantity and the radial and transverse components were to be measured. The two orientations of the elements of station 2 were not relative to the working point, but were mutually orthogonal. Amplitudes of the records shown in figures 4.3 and 4.4 are given in percent change of gauge resistance since the gauge factor of Ytterbium is uncertain.

4.4 Permeability investigation

A set of four sensitive pressure transducers was fielded in the emplacement hole and on the ground surface in a continuing investigation of the test site's permeability. The pressure histories thus obtained are presented in figure 4.5.

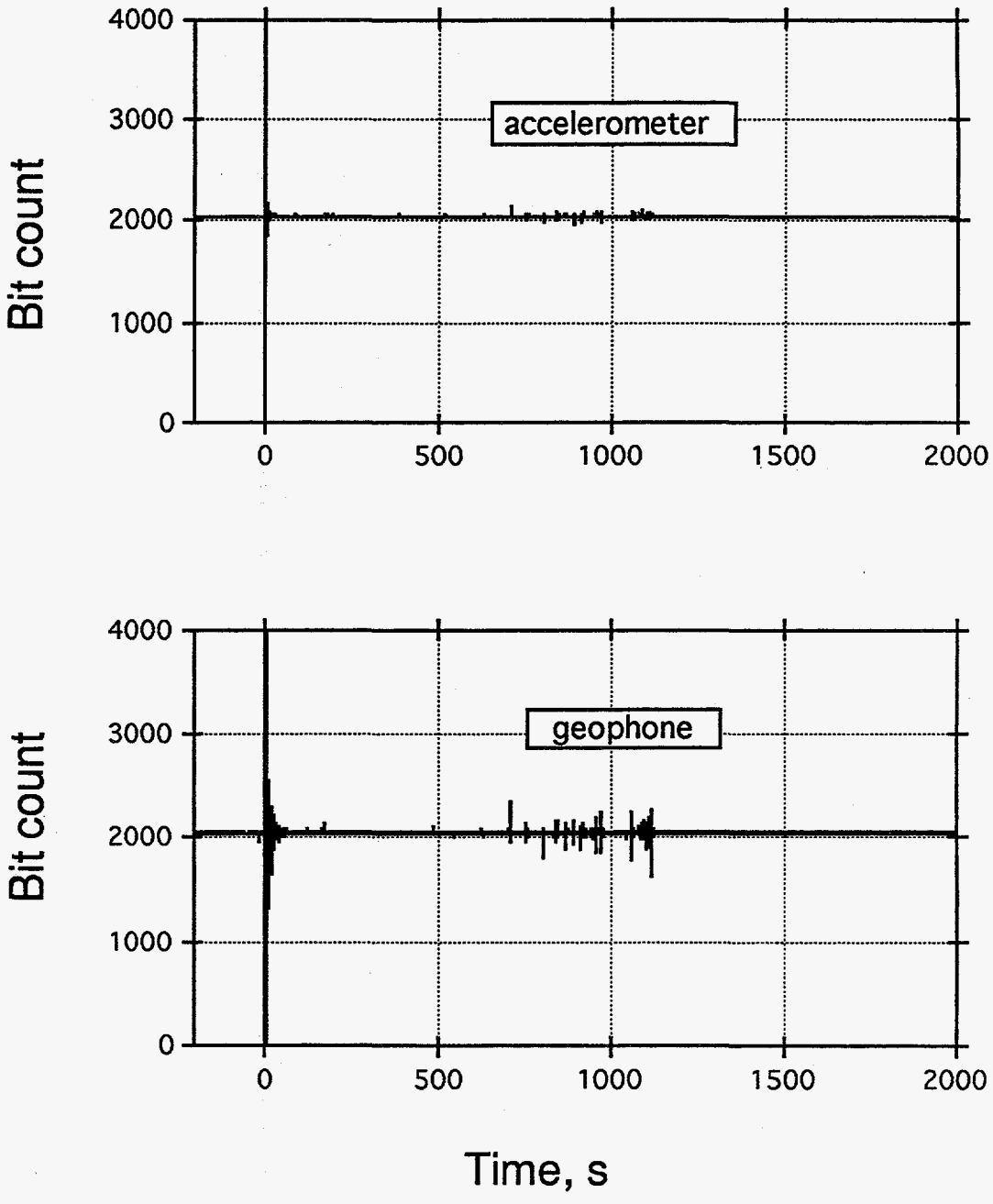

Figure 4.1 Data from the vertical geophone and sensitive accelerometer mounted in the ground surface at the recording trailer (station 62).

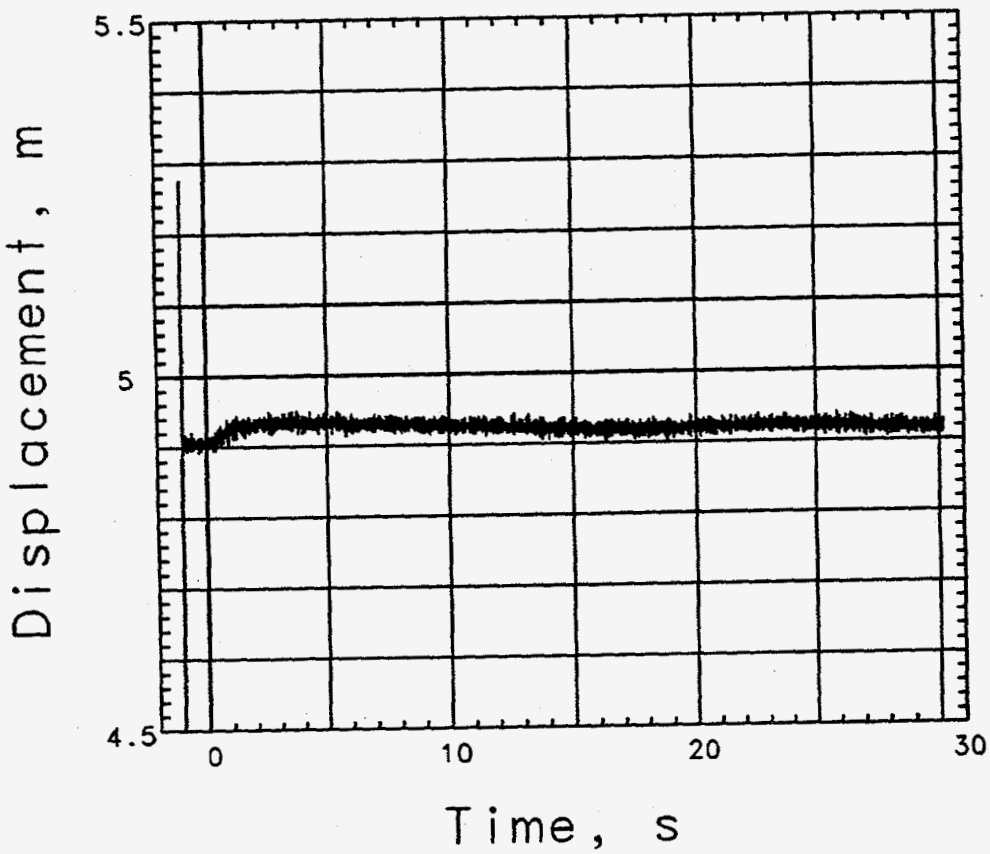

Figure 4.2 Displacement history of the gas sample hose.

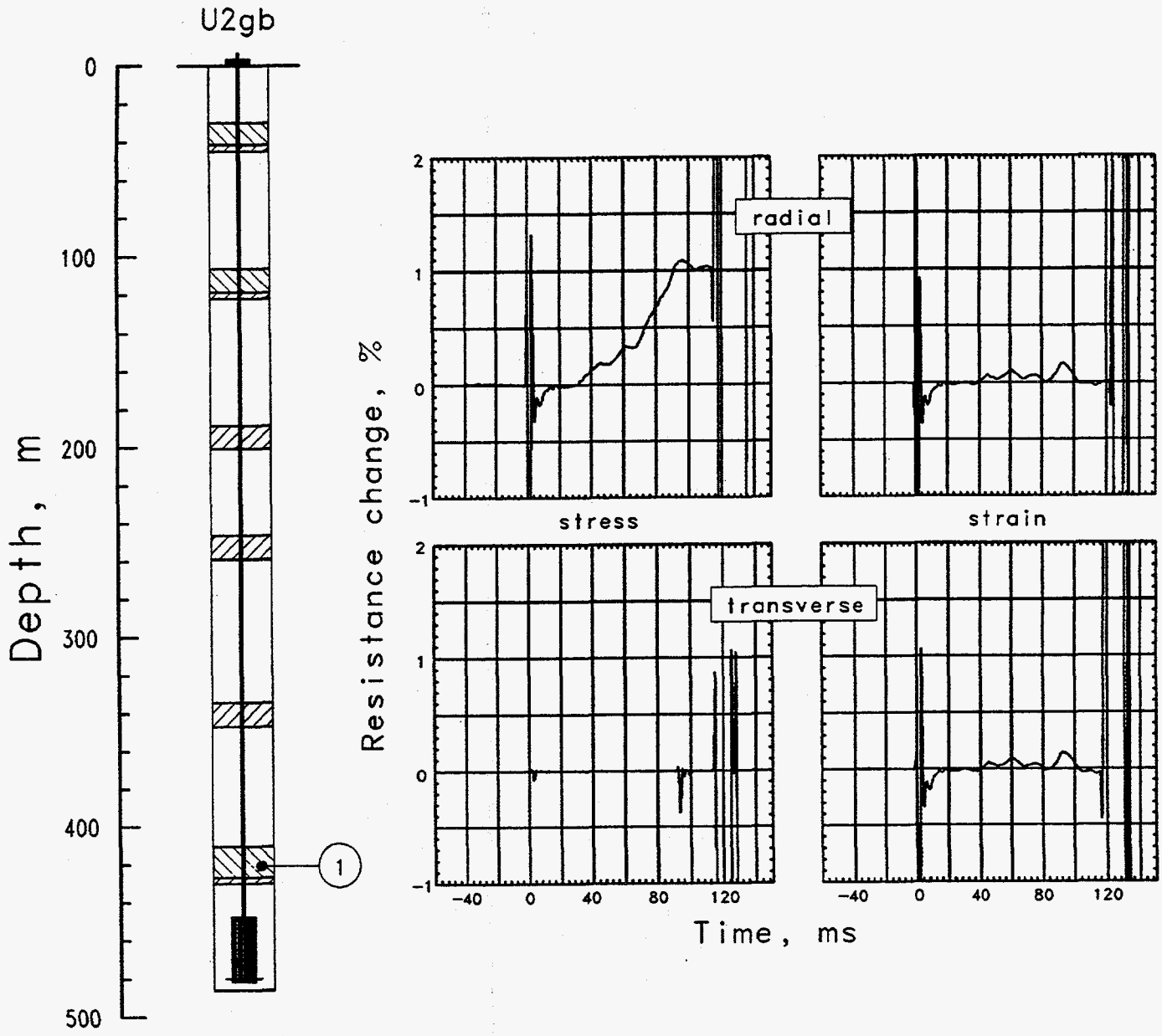

Figure 4.3 Stress and strain as measured in the bottom SGC plug (station 1, depth = 419.1 m). Amplitudes are in percent change of transducer resistance.

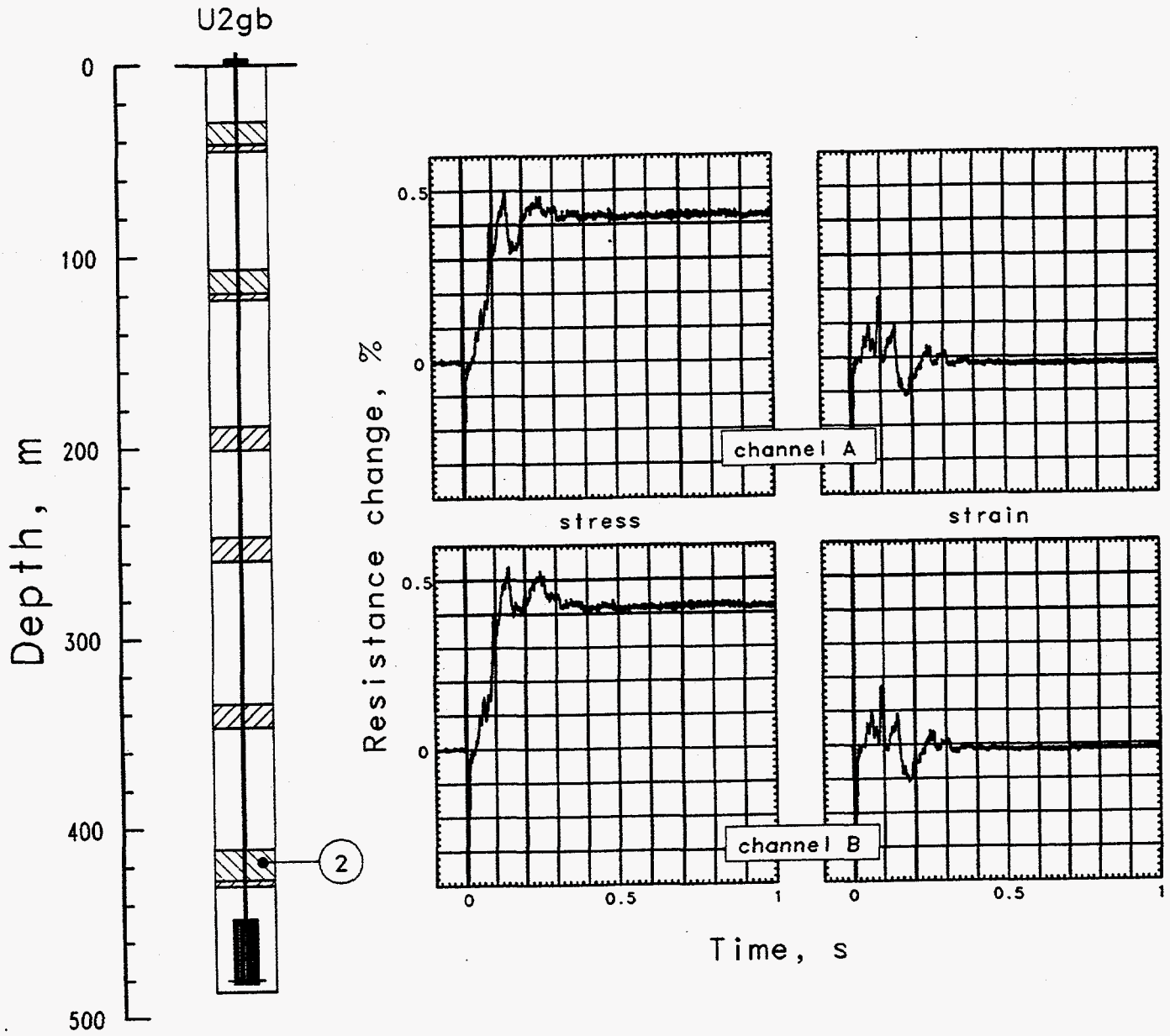

Figure 4.4 Stress and strain as measured in the bottom SGC plug (station 2, depth = 416.1 m). Amplitudes are in percent change of transducer resistance.

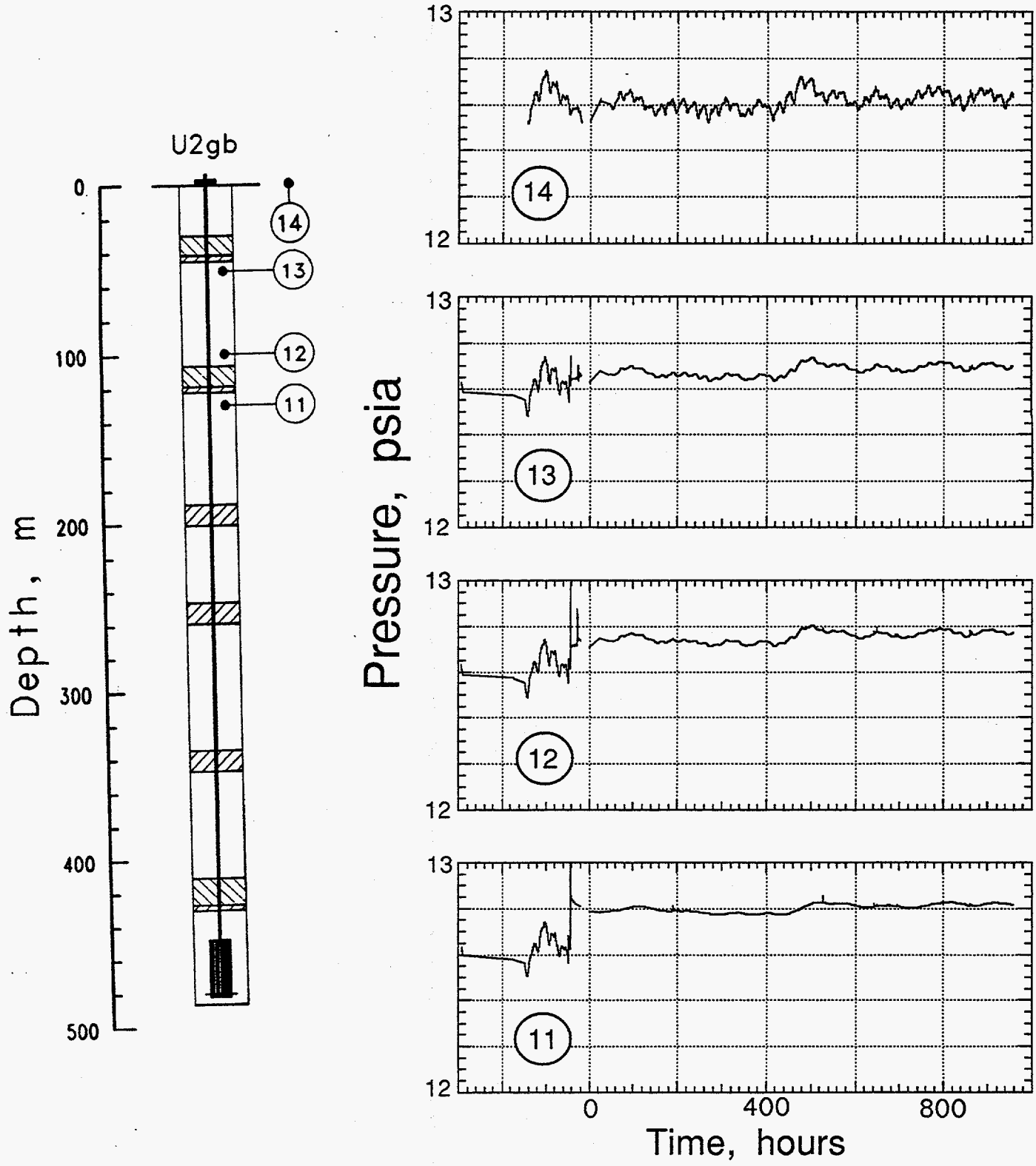

Figure 4.5 Sensitive pressure transducer outputs from the stemming column and the ground surface. Stations 11 - 13 show the effect of the stemming pour prior to the detonation at zero time.

References

1. Gayle Pawloski, "U2gb Site Characteristics Report", CP 85–83, Lawrence Livermore National Laboratory, Livermore, CA, September 20, 1985.

2. Alfred E. Burer, "Containment Report for U2gb (Revision)", Holmes & Narver, NTS:A2:86–38, May 23, 1986.

3. LLNL contacts for additional information: R. Heinle (CORRTEX data).

4. J. Kalinowski, T. Stubbs, L. Davies, and B. Hudson, "Recent stress gage developments", Range Commanders Council, Telemetry Group, 4-6 July, 1985, Monterey, California.

5. William G. Webb, "Special Measurements Final Engineering Report for PANAMINT, U2gb", EG&G, Energy Measurements, Las Vegas, NV, SM:86E–132–35.

6. William G. Webb, "Special Measurements Physics/Instrumentation for PANAMINT, U2gb, Revision "B" as built" EG&G, Energy Measurements, Las Vegas, NV, SM:85E–132–36.

Distribution:

LLNL

TID (11)	L-053
Test Program Library	L-045
Containment Vault	L-221
Burkhard, N.	L-221
Cooper, W.	L-049
Denny, M.	L-205
Dong, R.	L-140
Goldwire, H.	L-221
Heinle, R. (5)	L-221
Mara, G.	L-049
Moran, M.T.	L-777
Moss, W.	L-200
Olsen, C.	L-221
Patton, H,	L-205
Pawloski, G.	L-221
Rambo, J.	L-200
Roland, K.	L-221
Roth, B.	L-049
Valk, T.	L-154
Younker, L.	L-203

LANL

App, F.	F-659
Brunish, W.	F-659
Kunkle, T.	F-665
Trent, B.	F-664

Sandia

Chabai, A.	MS-1159
Smith, Carl W.	MS-1159

EG&G/AVO

Brown, T.	A-5
Gilmore, L.	A-1
Hatch, M.	A-5
Still, G.	A-5
Stubbs, T.	A-5

EG&G/NVO

Bellow, B.	N 13-20
Davies, L.	N 13-20
Moeller, A.	N 13-20
Robinson, R.	N 13-20
Webb, W.	N 13-20

DNA

Ristvet, B.

S-Cubed

Peterson, E.

Eastman Cherrington Environment
1640 Old Pecos Trail, Suite H
Santa Fe, NM 87504

Keller, C.